Anonymous Referee #1

This paper presents new pore water and sediments data from the Guaymas Basin in the Pacific, focusing on silicon and stable silicon isotopes, early diagenetic processes, and implications for silicon cycling in the oceans. The authors present new and high quality data, adding to a relatively sparse literature on the subject, and explore their interpretation with a model. The paper is very well-written and enjoyable to read. I have only a few comments and suggestions for where the methods and discussion could be expanded. As such, I am fully supportive of the publication of this manuscript with minor revisions.

Dear Reviewer,
Thank you very much for your positive feedback and the appreciation of our work. We mainly agree with the comments and suggestions you have raised and we will incorporate the requested changes in the manuscript, in case of a positive evaluation by the editor. Please find below our answers to your comments. All line numbers refer to the revised manuscript.

I would like to see some more detail in the methods and supplementary information.

1) Firstly, on page 6, line 182, the authors describe drying down the dissolved $bSiO_2$ samples prior to analysis. Could there have been any problems with loss of Si at this stage? Could the authors comment upon this and perhaps include yield data?

2) The described process of $bSiO_2$ digestion is a standard procedure following Reynolds et al. (2008) and Ehlert et al. (2012). Drying of the samples was shown by Ehlert et al. (2012) to have no effect on the Si isotopic composition of the samples. Additionally, Si is not volatile during evaporation and therefore fractionation affects not likely to occur.

3) The references and the comment on drying effects on the Si isotope composition were added in lines 179-181.

1) Secondly, I think that it would be incomplete not to mention the possibility of isotopic fractionation during dissolution of biogenic opal in section 4.1. I appreciate that this fractionation is poorly constrained, with very few studies that do not agree (Demarest et al., 2009; Egan et al., 2012, Wetzel et al., 2014). As such, I think that it's acceptable to say that we can assume that there is no appreciable fractionation, but the possibility should be included as a caveat.

2) As the referee mentions, we exclude significant effects on pore fluid $\delta^{30}Si_{pf}$ values, given the highly unconstrained and diverging results of former studies (Demarest et al., 2009; Egan et al., 2012; Wetzel et al., 2014). Nevertheless, the discussion of possible Si isotope fractionation in dependence of $bSiO_2$ dissolution is an important aspect.

3) We added a short paragraph in section 4.1 (lines 397-401) to address this caveat.

1) Thirdly, I would like to see more information about the modelling in the supplementary information. Such models are highly sensitive to the assumed dissolution rates of the involved phases. If any other group wanted to reconstruct this model, it would be challenging to do so without knowing exactly how e.g. the terrigenous phase dissolution rate profile parameter was quantified. Could the authors please include the actual equations used, linking depth in the sediment column with kinetic constants (i.e. the equations used to produce Figure S2)? I would like to know more about the sensitivity of the model to the assumed values of K/Al for the different phases. In particular, what is the sensitivity of the outputs to the ratio for the authigenic phase? It seems that the assumed value is for sediments from a very different environmental setting – can the authors

justify the use of values from the Gulf of Mexico for modelling the Guaymas Basin? How does precipitation at a hydrothermal site impact this ratio (section 4.3.2.)? I would suggest that the authors include a sensitivity experiment, perhaps with a few different profile plots for different (reasonable) assumed K/Al values, in the supplementary information. It might also be interesting to investigate the sensitivity of the model to variations in other 'constants' too, especially those that are poorly constrained or found to be variable in natural systems (e.g. the solubility of biogenic opal). Lastly, the caveats of the model are buried in the supplementary information, and I would like to see them more integrated into main text.

2) The assumed K/Al ratio is taken from sediments in the Amazon River delta, which are considered as the end product of reverse weathering reactions, given the complete conversion of the diatom frustule to authigenic aluminosilicates (Michalopoulos et al., 2000). The complete conversion of the diatom frustule is due to the input of highly reactive terrigenous minerals in the Amazon deltaic setting (Michalopoulos and Aller, 2004). The state of conversion of the diatom assemblage in the Guaymas Basin is difficult to assess, but similar K/Al ratios compared to the Amazon setting indicate a comparable high maturity state. At the hydrothermal site, the K/Al ratio is similar to the basin sites and indicates a similar state of conversion of the diatom frustule. Lower K/Al ratios and with that a lower maturity state of the diatom frustule were found in experiments by Loucaides et al. (2010). We agree that sensitivity tests will benefit the modelling outcomes and interpretation. For the modelling itself not K/Al but K/Si ratios from the same literature were used (see supplement) and modelling outcomes were recalculated for K/Al ratios. Therefore we conducted sensitivity tests with varying K/Si ratios and also sensitivity tests concerning the solubility constant of biogenic opal. The sensitivity tests showed that lower K/Si ratios (and with that lower K/Al ratios) could not reproduce the measured K/Al ratios in the OMZ. Therefore, we conclude that the assumed K/Al ratios of Michalopoulos et al. (2000) are valid also for authigenic minerals in the Guaymas OMZ.

3) Sensitivity tests and the outcomes were added in the supplement. Also, the caveats of the model were moved to the main text in lines 550-553.

Additional sensitivity tests regarding the solubility of biogenic opal, the $\delta^{30}Si$ values of the dissolving terrigenous phase and the Si isotope fractionation during authigenic clay formation were conducted following also the recommendations by reviewer #3.

2) I also think that there are aspects of the discussion that could be expanded upon to utilize the full range of data available.

1) Firstly, the XRD data is not referred to at all the discussion. How does the clay mineralogy inform on the discussion? Does it help with constraining reverse weathering reactions and/or, for example, the potential shifts in K/Al within the sediments (e.g. section 4.3.3.)?

2) In section 4.3.2 of the original manuscript we actually used the XRD data on amorphous SiO_2 in the discussion of hydrothermal processes (lines 474-476). However, we made no attempt to use XRD data for the detection of reverse weathering reactions because it is difficult to distinguish authigenic clays formed during these reactions from terrigenous clays that are very abundant in our study area. For this reason, we did in fact not analyze the OMZ sediments with XRD so that we are unfortunately not able to follow this reviewer recommendation.

1) Secondly, I also do not think that the pore water trace metals are used to their full potential. For example, are there any trends in the [Fe] data from the hydrothermal site to suggest that Fe-cycling could be impacting silicon isotope fractionation? (section 4.3.3.)

2) Unfortunately, the available data set is too scarce to identify possible Si isotope fractionation induced by Fe. Experimental results by Zheng et al. (2016) indicate that $\delta^{30}Si$ values should increase with the Fe/Si ratio in the solids and pore fluids. We see a similar trend in our data from the basin sites and hydrothermal site indicating a possible Fe-induced fractionation (see figure below). Data from the OMZ site, in contrast, deviate from this apparent trend (however, only based on two data points) and show lower $\delta^{30}Si_{pf}$ values as what would be expected regarding the Fe/Si ratio. This could be related to the likely one step fractionation during Fe-Si co-precipitation at the hydrothermal site and the existence of multiple Fe redox cycles inducing Si dissolution and re-precipitation and with that multiple fractionation steps at the OMZ site (lines 507-510). Furthermore, any Fe-induced Si isotope fractionation is likely superimposed by the dissolution of terrigenous clays as shown by the reactive transport model. Natural Fe-induced Si isotope fractionation needs further investigation in future studies in order to be able to identify magnitudes of fractionation if other fractionating processes take place simultaneously.

3) We added the figure below and a short discussion on Fe-induced fractionation to the supplementary information in order to address the reviewer's comment (reference in the main text in line 510).

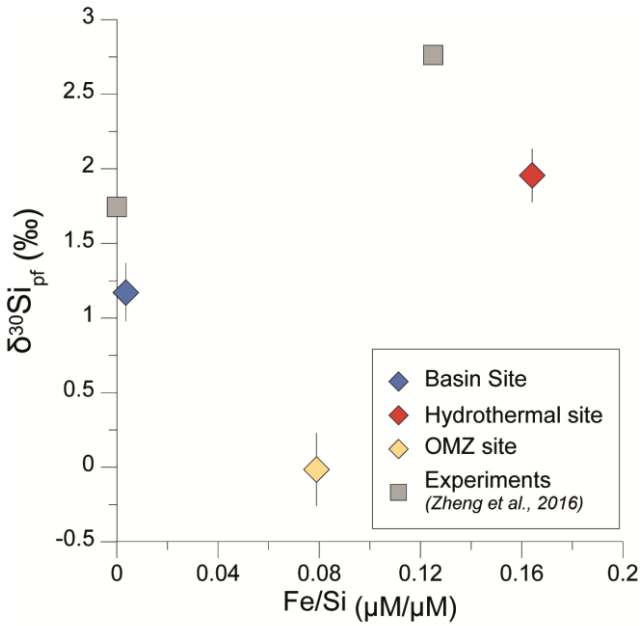

Additional figure to reviewer comment 2-2. Si isotope fractionation in dependence of the Fe/Si ratio in the fluids. Experimental data from Zheng et al. (2016) are shown for comparison.

3) Other minor comments:

1) I'd suggest that the authors should be consistent and use either "pore fluids" or "pore waters" throughout the text.

2+3) We used "pore fluids" throughout the text.

1) Line 32: Please change "the only other marine setting where Si isotopes have been investigated to constrain early diagenetic processes" to "the only other OMZ marine setting where Si isotopes have been investigated to constrain early diagenetic processes", to acknowledge that other marine settings have been investigated (e.g. Ng et al., 2020).

2+3) We added 'OMZ' to the sentence (line 32) and previous studies conducted in other marine settings are discussed in lines 89-96.

Referee #2 , Jill Sutton

The manuscript by Geilert and co-authors presents stable silicon isotope data obtained from pore fluid, water column, hydrothermal plume, and sediment samples at several different sites in the Guaymas Basin. The authors present the geochemical differences observed at these different sites and discuss the implications of processes, such as early diagenesis, on the cycling of Si in the marine environment. The data are of high quality and the authors have done an excellent job at interpreting and presenting their data. The manuscript is timely and worthy of publication in Biogeosciences. This is the second time that I have reviewed this manuscript (first time was with GCA), and I have very few additional suggestions to make, and only of an editorial manner.

Dear Jill Sutton,
Thank you very much for your positive evaluation and the valuable feedback and comments on our manuscript. We will incorporate the changes you propose in case of a positive evaluation by the editor. All line numbers refer to the revised manuscript.

1) Lines 13 and 44 (for example) – Can the authors please check their usage of the definition of Si throughout the text? Here the authors describe silica as Si (line 13) but also silicon as Si. I would prefer that the authors of the manuscript use Si to describe silicon and SiO2 for silica (consistent with the other abbreviations used throughout the text).

2+3) We used the abbreviation Si for silicon and SiO_2 for silica throughout the revised text.

1) Line 226 – please change "insignificant" to "unimportant".

2+3) We changed the word accordingly (line 229).

1) Throughout – it is De La Rocha (and not de la Rocha). Varela (2004) should be Varela et al. 2004

2+3) We changed the references accordingly.

Referee #3, Damien Cardinal

This manuscript presents new interesting silicon isotope data from sediment pore fluids (d30Sipf) in different marine environments from Guyamas Basin and Gulf of California. The data are of high quality and include d30Sipf from sites located into Oxygen Minimum Zone or under the influence of hydrothermal vents both of which are particularly new in terms of Si isotopic system. This work

certainly deserves publication in Biogeosciences after improvement / clarification of some parts of the discussion. I have compiled my concerns under the scope of the three main concerns below, which do not necessarily imply much work to be implemented.

Dear Damien Cardinal,
Thank you very much for your positive feedback and valuable comments to our manuscript. We are happy to discuss and incorporate the aspects you raised below in a revised version of this manuscript in case of a positive evaluation by the editor. All line numbers refer to the revised manuscript.

1) The role of **bioturbation** is never mentioned in the main text (e.g. 76-77) despite it is an important process in the upper cm (cf. e.g. Rabouille et al. 1997 for Si). It is however a parameter of the model. However, the model is used only for the OMZ site where we could expect null or negligible bioturbation because it is very low oxygen environments. How could bioturbation not affect the porefluid profiles of the other sites? In contrast why this has been considered at the OMZ site? Some discussion should be added in the main text.

2) We agree that bioturbation and bioirrigation and with that the mixing of upper sediments and pore fluids are important processes which were not mentioned in the main text of the manuscript. Bioturbation is expected to have the largest impact within the upper ~10 cm below seafloor (cmbsf) and bioirrigation within the upper ~20 cmbsf. However, the homogeneity of the pore fluid $\delta^{30}Si_{pf}$ values with depth (see lines 427-429) suggests that the effects of bioturbation/bioirrigation on pore fluid composition are largely compensated by fast reactions inducing rapid isotope exchange. Unfortunately, we have no independent data to quantify rates of bioturbation and bioirrigation in our study area. Therefore, we limited the modelling to the OMZ site where the biogenic mixing proceeds at very low rates due to the absence of large benthic biota.

3) Nevertheless, we will briefly discuss the potential effects of bioturbation/bioirrigation at the hydrothermal and basin sites in section 4.2 (429-433).

Identification of minerals under or over saturated in the pf is not sufficiently directly addressed in the discussion. See e.g.:

1) 457-459. It is unclear how "*Si concentrations lower than amorphous Si and quartz solubilities, indicating precipitation of the respective mineral phase during pore fluid ascent*". If the DSipf is lower than equilibrium concentration, then Si should rather dissolve than precipitate.

2+3) The sentence was rephrased according to calculated saturation indices (see comment below).

1) What are the minerals which are actually oversaturated in pf? Why saturation indexes of primary and secondary minerals have not been calculated e.g. using data of Table 1S?

2) We calculated saturation indices for pure silica phases (amorphous SiO_2, quartz) using the program and databases of PHREEQC (Parkhurst and Appelo, 1999). However, no saturation indices can be calculated for the most important precipitating phase discussed in this manuscript, namely authigenic aluminosilicates because we have no data on the dissolved Al concentrations and in-situ pH values of the pore fluids. For the hydrothermal site, saturation indices show that quartz is supersaturated and amorphous silica is close to saturation. Consequently, quartz can precipitate directly from pore fluids at present. However, due to the dynamics of hydrothermal systems, this can be subject to changes and supersaturation of amorphous silica is likely to be obtained occasionally, due to the ascent of Si enriched fluids from greater depth as indicated by the presence of amorphous silica cement in the hydrothermally affected sediments.

3) We added a paragraph discussing saturation indices in section 4.3.2, lines 469-473.

1) 480-481 and 499-512. Could dissolution of primary minerals (e.g. feldspars) supply DSi in pf? If not, justify why this can be ruled out. Even though primary minerals are less prone to dissolution than clays, they are likely to be undersaturated in the pf and may have some impact on DSi and d30Sipf.

2) It is true that reactive primary minerals like feldspars may dissolve in the pore fluids (e.g. Singer, 1980; Wilson, 2004). However, the $\delta^{30}Si$ values of feldspars are rather high compared to clays with an average of -0.17‰ (Georg et al., 2009; Savage et al., 2011) and their dissolution alone cannot be responsible for the shift to low $\delta^{30}Si_{pf}$ values in the OMZ (see also answer to comment #3 Modelling). During changing environmental conditions immature clays like e.g. chlorite can transform and dissolve (Singer, 1980), often accelerated by organic ligands and iron reduction in the clay structure (Anderson and Raiswell, 2004; and lines 522-531). We agree, that primary mineral dissolution is likely to take place, however, superimposed by clay dissolution, shifting OMZ pore fluid $\delta^{30}Si_{pf}$ to the observed low values. We conducted a sensitivity test considering feldspar dissolution (see also answer to comment #3). Our results indicate that feldspar dissolution alone cannot create the low $\delta^{30}Si_{pf}$ values in the OMZ.

3) We added the results of this sensitivity test to the supplement and addressed the results and a discussion on primary silicate dissolution in the main text lines 517-520.

1) Why there is no mineral data on the OMZ core (Table 2S) despite this is the site for which the discussion is the most developed?

2) We agree that XRD data for the OMZ site would be helpful and could add another argument for clay dissolution and/ or authigenic mineral precipitation. Unfortunately, by the time when the XRD analyses were conducted, the focus of the study was not on the OMZ site. Only in the course of the manuscript writing and handling, the focus shifted to the OMZ site. However, we also think that the recognition of authigenic mineral formation is rather difficult to decipher based on XRD data (see comment to reviewer #1, point 2-1) and would not have supported the discussion to a large degree because the clay mineralogy of the OMZ site is probably dominated by riverine clays that are very abundant in our study area and complicate the detection of authigenic clay formation. We show, that we can fully explain the observed low $\delta^{30}Si_{pf}$ values by clay dissolution. The interpretation is additionally supported by our modeling and K/Al data.

1) Fig.3. What is the uncertainty we have on Si concentration for dissolved bSi to build the mixing line that has been taken at equilibrium (900 uM)? The equilbrium concentration is theoretical however why would the dissolution of bSiO2 be at equilibrium and give Sipf at 900 uM for the end-member chosen in Fig. 3?

2) The assumed $bSiO_2$ equilibrium concentration of 900µM is an experimentally determined value for siliceous sediment (Van Cappellen and Qiu, 1997; see also lines 392-394). This concentration value takes into account early diagenetic reactions like the incorporation of Al in the diatom frustule. This diagenesis-affected concentration value is lower than equilibrium concentrations of acid-cleaned $bSiO_2$ (see Van Cappellen and Qiu, 1997 and references therein). We agree, however, that equilibrium concentrations might vary from site to site depending on the maturity of the diatom frustules.

3)

3) Therefore we added an uncertainty of ± 150µM Si to the assumed concentration (c.f. Van Cappellen and Qiu, 1997) and added a range in Fig. 3 and a comment in the caption. Note that the uncertainty of the equilibrium solubility of $bSiO_2$ has only minor impact on the calculated mixing curves.

3) Model set up from line 524 and in the Supplement. The sensitivity of the model to its main hypotheses is not sufficiently discussed in the main text and there is a lack of justification for some of its core parameters.

1) The average value of clay used in the model is -2 pmil and reference to Frings et al. (2016) is given for this. However, average clays in Frings et al. is not at -2 pmil. I'm not sure it is actually calculated, but from the figure, it should be more between -1.5 and -1 pmil. This would be also consistent with the review of Sutton et al. (2018) In which the world average value of secondary minerals is at -1.08 pmil. Similarly, in Bayon et al. (2018) the average clay d30Si from river sediment fluctuate from -1.5 to -0.32 pmil depending on climatic regimes. How does it affect model outputs when using a more realistic d30Si of clay (i.e. -1.5 or -1 pmil) and/or propagate the uncertainty of this value? In any case, the use of -2 pmil as average clay value is not properly justified.

2) The terrigenous clays brought to the basin by river discharge are likely phyllosilicates like kaolinites (e.g. Georg et al., 2006; Frings et al., 2014) which are associated with lower $\delta^{30}Si$ values caused by the larger Si isotope fractionation factor associated with single layer phyllosilicates (Opfergelt et al., 2012). Therefore, it is valid to assume a clay $\delta^{30}Si$ value of -2‰. However, we agree that the reference to Frings et al. (2016) is not sufficiently explaining this assumption and we agree that a sensitive test of the model taking into account various clay $\delta^{30}Si$ values will improve the manuscript and the significance of the model results. Therefore, we conducted sensitivity tests for clay $\delta^{30}Si$ values covering a range of -2 to -1 ‰ and for primary mineral dissolution with $\delta^{30}Si$ values close to zero. Results of the sensitivity tests show that dissolution of terrigenous material with higher $\delta^{30}Si$ values than -2‰ cannot reproduce the measured $\delta^{30}Si$ values in the OMZ pore fluids. Only if the fractionation factor is lowered to -1‰, terrigenous material with $\delta^{30}Si$ values of -1.7‰ can produce the observed values (see also comment below). In conclusion, the dissolving terrigenous phase is strongly depleted in ^{30}Si and only clay dissolution can produce the low pore fluid $\delta^{30}Si$ values in the OMZ.

3) We added these sensitivity tests to the supplement and refer to the results in the main text (lines 557-559 and 574-578).

1) Similarly uncertainty on the -2 pmil for the isotopic fractionation during precipitation of authigenic clay should be discussed and taken into account

2) We agree that the model will benefit from sensitivity tests concerning the Si isotope fractionation factor. We conducted sensitivity tests applying $\Delta^{30}Si$ values of -1‰ and 0‰ following Opfergelt et al. (2012). A fractionation factor of -1 ‰ reproduces the measured pore fluid $\delta^{30}Si$ values in the OMZ if a terrigenous phase with slightly higher $\delta^{30}Si$ values (-1.7‰ compared to -2‰) dissolves.

3) We included the outcomes of this sensitivity test in the supplement and refer to the results in the main text (lines 557-559 and 574-578).

1) Role of bioturbation in the model for the OMZ (cf. first comment)

2) Bioturbation is of minor importance for the OMZ given the absence of large benthic biota under anoxic conditions. The model incorporates a small bioturbation coefficient. However, the depth of the bioturbated layer is limited to 1 cm considering the absence of burrowing organisms.

1) Could the model be applied to the other sites, e.g. basin?

2) In contrast to the OMZ, the other sites are likely influenced by bioturbation and bioirrigation even if the impact on pore fluid $\delta^{30}Si_{pf}$ values appears to be compensated by fast reactions (see answer to comment #1). Unfortunately, we have no independent data to quantify rates of bioturbation and bioirrigation in our study area. Therefore, we limited the modelling to the OMZ site where the biogenic mixing proceeds at very low rates due to the absence of large benthic biota.

Minor comments

1) Throughout the ms, better use heavier / lighter than higher / lower when reference is made to isotopic composition.

2) In the original manuscript we used the expression higher and lower when referring to $\delta^{30}Si$ values, as a value by its nature cannot be light or heavy. We used the expression lighter and heavier when referring to isotopic compositions (e.g. in line 404).

1) 176 : « *The bSiO2 samples were stored in Milli-Q water* » Does it mean that once separated by Morley et al. (2004) method, the bSiO2 samples were kept in water ? For how long? Dissolution could have occurred with some isotopic fractionation?

2) The cleaned diatom samples were stored in MQ-water for several days. Dissolution of $bSiO_2$ is unlikely given that the pH of the MQ-water (~ 5) is not favoring $bSiO_2$ dissolution. Dissolution rates increase quickly between pH 9 to 10.7 (Iler, 1979) and that is also the reason why digestion of the $bSiO_2$ samples is conducted in an alkaline medium. Additionally, the water-$bSiO_2$ mixture was transferred to a Teflon vial for further handling, so in the unlikely case of fractionation effects during dissolution, the bulk would have been further processed and no isotopic signal was lost.

1) 238. Typo, 2 times « and »

2+3) We removed the second 'and'.

1) 301 Is it worth keeping MUC-22-04 whose bottom SW has been contaminated? (likely by surface SW)

2) Because of completeness of the results section, we prefer to leave the sample MUC-22-04 in and report the Si concentration and $\delta^{30}Si$ values.

1) 366: the kinetics of reverse weathering is poorly known, especially in situ and is certainly not immediate. So do not to use such wording « *as soon as Si is released (...), it reprecipitates* ». Moreover not all Si reprecipitates, otherwise there won't be more DSi in pore fluids than in bottom water (indeed in their previous work, Elhert et al. 2016 have quantified that only 24% of dissolved bSi reprecipitates). This sentence needs to be corrected.

3) We corrected the sentence accordingly (lines 369-372).

1) 371-372 From the three references cited here, only Elhert et al. 2016 has estimated fractionation factors for reverse weathering, the other two refer to continental weathering (Georg et al., 2006 and Opfegerlt et al., 2013). Remove them or specify it since this sentence is misleading.

3) We removed the references *Georg et al., 2009* and *Opfergelt et al., 2013* (lines 374-375).

1) 395-398. Sentence unclear / grammatically incorrect

3) We rewrote the sentence (lines 403-406).

1) 397. At least one reference should be cited for Si isotope fractionation during bSi dissolution (e.g. DeMarest et al., 2009).

2+3) We discussed the potential impact on Si isotope fractionation during dissolution and add the following references: Demarest et al., 2009, Egan et al., 2012, Wetzel et al., 2014 (see also comment to reviewer #1) (lines 397-401).

1) 440-441. This sentence is too affirmative given the level of discussion at this stage of the ms. It could be changed to e.g. “Thus, at Basin sites both K/Al ratios of sediments and the heavier d30Sipf are in agreement to recognise bSi dissolution followed by authigenic clay formation as significant processes taking place”.

3) We rephrased the sentence accordingly (lines 450-452).

1) 527: typo in isotope

3) The typo was corrected.

1) Table S5 Typo « auf »

3) The typo was corrected.

1) Fig. 5. It should be mentioned in the caption that Fig. 5b is from another study (Ehlert et al. 2016?)

3) The reference *Ehlert et al., 2016* was included in the caption of Fig. 5.

1) Fig. 6. Need to define red and black dashed line in the caption without having to go through the text in the ms.

3) The definitions of the red and black dashed lines were included in the caption.

References to the answer letter

Anderson T. F. and Raiswell R. (2004) SOURCES AND MECHANISMS FOR THE ENRICHMENT OF HIGHLY REACTIVE IRON IN EUXINIC BLACK SEA SEDIMENTS. *Am. J. Sci.* **304**, 203–233.

Van Cappellen P. and Qiu L. Q. (1997) Biogenic silica dissolution in sediments of the Southern Ocean.1. Solubility. *Deep. Res. Part Ii-Topical Stud. Oceanogr.* **44**, 1109–1128.

Ehlert C., Grasse P., Mollier-Vogel E., Böschen T., Franz J., de Souza G. F., Reynolds B. C., Stramma L. and Frank M. (2012) Factors controlling the silicon isotope distribution in waters and surface sediments of the Peruvian coastal upwelling. *Geochim. Cosmochim. Acta* **99**, 128–145.

Frings P. J., Clymans W., Fontorbe G., De La Rocha C. L. and Conley D. J. (2016) The continental Si cycle and its impact on the ocean Si isotope budget. *Chem. Geol.* **425**, 12–36. Available at: http://dx.doi.org/10.1016/j.chemgeo.2016.01.020.

Frings P. J., Rocha C. D. La, Struyf E., Pelt D. Van, Schoelynck J., Hudson M. M., Gondwe M. J., Wolski P., Mosimane K., Gray W., Schaller J. and Conley D. J. (2014) Tracing silicon cycling in the Okavango Delta, a sub-tropical flood-pulse wetland using silicon isotopes. *Geochim. Cosmochim. Acta* **142**, 132–148. Available at: http://www.sciencedirect.com/science/article/pii/S0016703714004694.

Georg R. B., Reynolds B. C., Frank M. and Halliday a. N. (2006) Mechanisms controlling the silicon isotopic compositions of river waters. *Earth Planet. Sci. Lett.* **249**, 290–306.

Georg R. B., Zhu C., Reynolds B. C. and Halliday A. N. (2009) Stable silicon isotopes of groundwater, feldspars, and clay coatings in the Navajo Sandstone aquifer, Black Mesa, Arizona, USA. *Geochim. Cosmochim. Acta* **73**, 2229–2241. Available at: http://dx.doi.org/10.1016/j.gca.2009.02.005.

Iler R. K. (1979) *The Chemistry of Silica*., John Wiley & Sons Inc, New York.

Loucaides S., Michalopoulos P., Presti M., Koning E., Behrends T. and Van Cappellen P. (2010) Seawater-mediated interactions between diatomaceous silica and terrigenous sediments: Results from long-term incubation experiments. *Chem. Geol.* **270**, 68–79. Available at: http://dx.doi.org/10.1016/j.chemgeo.2009.11.006.

Michalopoulos P. and Aller R. C. (2004) Early diagenesis of biogenic silica in the Amazon delta: Alteration, authigenic clay formation, and storage. *Geochim. Cosmochim. Acta* **68**, 1061–1085.

Michalopoulos P., Aller R. C. and Reeder R. J. (2000) Conversion of diatoms to clays during early diagenesis in tropical, continental shell muds. *Geology* **28**, 1095–1098.

Opfergelt S., Georg R. B., Delvaux B., Cabidoche Y. M., Burton K. W. and Halliday a. N. (2012) Silicon isotopes and the tracing of desilication in volcanic soil weathering sequences, Guadeloupe. *Chem. Geol.* **326**–**327**, 113–122. Available at: http://dx.doi.org/10.1016/j.chemgeo.2012.07.032.

Parkhurst B. D. L. and Appelo C. a J. (1999) User's Guide To PHREEQC (version 2) — a Computer Program for Speciation, and Inverse Geochemical Calculations. *Exch. Organ. Behav. Teach. J.* **D**, 326. Available at: http://downloads.openchannelsoftware.org/PHREEQC/manual.pdf.

Reynolds B. C., Frank M. and Halliday A. N. (2008) Evidence for a major change in silicon cycling in the subarctic North Pacific at 2 . 73 Ma. *Paleoceanography* **23(PA4219)**.

Savage P. S., Georg R. B., Williams H. M., Burton K. W. and Halliday A. N. (2011) Silicon isotope fractionation during magmatic differentiation. *Geochim. Cosmochim. Acta* **75**, 6124–6139.

Singer A. (1980) The Paleoclimatic Interpretation of Clay Minerals in Soils and Weathering Profiles. *Earth-Science Rev.* **15**, 303–326.

Wilson M. J. (2004) Weathering of the primary rock-forming minerals: processes, products and rates. *Clay Miner.* **39**, 233–266.

Zheng X., Beard B. L., Reddy T. R., Roden E. E. and Johnson C. M. (2016) Abiologic silicon isotope fractionation between aqueous Si and Fe (III) -Si gel in simulated Archean seawater : Implications for Si isotope records in Precambrian sedimentary rocks. *Geochemica Cosmochim. Acta* **187**, 102–122.

Impact of ambient conditions on the Si isotope fractionation in marine pore fluids during early diagenesis

Sonja Geilert[1], Patricia Grasse[1], Kristin Doering[1,2], Klaus Wallmann[1], Claudia Ehlert[3], Florian Scholz[1], Martin Frank[1], Mark Schmidt[1], Christian Hensen[1]

[1]GEOMAR Helmholtz Centre for Ocean Research Kiel, Wischhofstr. 1-3, 24148 Kiel, Germany
[2]Department of Oceanography, Dalhousie University, Halifax, Canada
[3]Marine Isotope Geochemistry, ICBM, University of Oldenburg, Germany

ABSTRACT

Benthic fluxes of dissolved ~~silica~~ silicon (Si) from sediments into the water column are driven by the dissolution of biogenic silica ($bSiO_2$) and terrigenous Si minerals and modulated by the precipitation of authigenic Si phases. Each of these processes has a specific effect on the isotopic composition of ~~silica~~ silicon dissolved in sediment pore ~~waters~~ fluids such that the determination of pore fluid~~water~~ $\delta^{30}Si$ values can help to decipher the complex Si cycle in surface sediments. In this study, the $\delta^{30}Si$ signatures of pore fluids and $bSiO_2$ in the Guaymas Basin (Gulf of California) were analyzed, which is characterized by high $bSiO_2$ accumulation and hydrothermal activity. The $\delta^{30}Si$ signatures were investigated in the deep basin, in the vicinity of a hydrothermal vent field, and at an anoxic site located within the pronounced oxygen minimum zone (OMZ). The pore fluid $\delta^{30}Si_{pf}$ signatures differ significantly depending on the ambient conditions. Within the basin, $\delta^{30}Si_{pf}$ is essentially uniform averaging +1.2±0.1‰ (1SD). Pore fluid $\delta^{30}Si_{pf}$ values from within the OMZ are significantly lower (0.0±0.5‰, 1SD), while pore fluids close to the hydrothermal vent field are higher (+2.0±0.2‰, 1SD). Reactive transport modelling results show that the $\delta^{30}Si_{pf}$ is mainly controlled by silica dissolution ($bSiO_2$ and terrigenous phases) and Si precipitation (authigenic aluminosilicates). Precipitation processes cause a shift to high pore fluid $\delta^{30}Si_{pf}$ signatures, most pronounced at the hydrothermal site. Within the OMZ however, additional dissolution of isotopically depleted Si minerals (e.g. clays) facilitated by high mass accumulation rates of terrigenous material (MAR_{terr}) is required to promote the low $\delta^{30}Si_{pf}$ signatures while precipitation of authigenic aluminosilicates seems to be hampered by high water/rock ratios. Guaymas OMZ $\delta^{30}Si_{pf}$ values are markedly different from those of the Peruvian OMZ, the only other marine OMZ setting where Si isotopes have been investigated to constrain early diagenetic processes. These differences highlight the fact that $\delta^{30}Si_{pf}$ signals in OMZs worldwide are not alike and each setting can result in a range of $\delta^{30}Si_{pf}$ values as a function of the

environmental conditions. We conclude that the benthic ~~silica~~ silicon cycle is more complex than previously thought and that additional Si isotope studies are needed to decipher the controls on Si turnover in marine sediment and the role of sediments in the marine ~~silica~~ silicon cycle.

KEYWORDS: Si isotopes, reverse weathering, hydrothermal system, oxygen minimum zone, environmental conditions

1. INTRODUCTION

Silicon (Si) is one of the key macronutrients in the ocean mainly utilized by siliceous organisms such as diatoms, radiolarians or sponges (see recent review by Sutton et al., 2018). The marine Si cycle is closely linked to the carbon (C) cycle by marine siliceous organisms, which transport C to the sediment and thus exert a strong control on C export from the atmosphere impacting present and past climate (e.g. Lewin, 1961; Tréguer and Pondaven, 2000; Tréguer and De La Rocha, 2013; and recent reviews by Frings et al., 2016 and Sutton et al., 2018). Studies of Si isotopes ($\delta^{30}Si$) have revealed complex uptake and dissolution processes of siliceous organisms, which have a dominant control on the $\delta^{30}Si$ distribution in ocean waters (e.g. ~~de~~ De ~~la~~ La Rocha et al., 1997; Varela et al.,~~,~~ 2004; Cardinal et al., 2005; Beucher et al., 2008; Fripiat et al., 2011; Ehlert et al., 2012; Grasse et al., 2013; Sutton et al., 2013; de Souza et al., 2014, 2015). Diatoms constitute the largest part of the Si cycling fluxes in the ocean (Ragueneau et al., 2000) and discriminate between its isotopes during Si uptake, whereby the light isotopes are preferentially incorporated into the diatom frustules (e.g. ~~de~~ De ~~la~~ La Rocha et al., 1997). Si isotope fractionation during ~~silica~~ Si uptake is dependent on e.g. the diatom species, the availability of Fe, and the degree of Si~~silica~~ utilization. Fractionation factors between -0.5 and -2.1‰ have been derived from regional water mass mixing and laboratory studies (~~de~~ De ~~la~~ La Rocha et al., 1997; Varela et al., 2004; Cardinal et al., 2005; Beucher et al., 2008; Sutton et al., 2013; Meyerink et al., 2017).

After a planktonic bloom whereupon the nutrients are exhausted, biogenic silica ($bSiO_2$, mainly diatoms) sinks through the ocean, partially dissolves and accumulates on the seafloor, where its preservation and recycling is controlled by dissolution and Si re-precipitation processes. The dissolution of $bSiO_2$ mainly controls the accumulation of silicic acid ($Si(OH)_4$) in pore fluids, although the in-situ concentration remains below the equilibrium concentration of dissolved $bSiO_2$, which has been explained by simultaneous formation of authigenic silicates (e.g. McManus et al., 1995; Van Cappellen and Qiu, 1997a, b; Rickert et al., 2002). This process is termed reverse weathering given that the authigenic precipitates are rich in seawater-derived cations, like Na, K or Mg (Mackenzie et al., 1981; Michalopoulos and Aller, 1995). Experimental studies of $bSiO_2$ dissolution kinetics revealed

a dependence of the $bSiO_2$ reactivity on sediment depth as well as the ratio between terrigenous material and $bSiO_2$ (Michalopoulos and Aller, 1995; Van Cappellen and Qiu, 1997a, b; Dixit et al., 2001; Rickert et al., 2002). Marine weathering of terrigenous material (primary silicates like feldspars and secondary silicates like clays), was found to release cations such as aluminum (Al) or iron (Fe), which reduce the solubility and dissolution rate of $bSiO_2$ and induce aluminosilicate precipitation (Michalopoulos and Aller, 1995; Van Cappellen and Qiu, 1997a, b; Michalopoulos et al., 2000; Dixit et al., 2001; Rickert et al., 2002; Loucaides et al., 2010). The accumulation of Si in pore fluids and the Si reflux into bottom waters are controlled by three interdependent processes, namely: opal dissolution, dissolution of terrigenous solids, precipitation of authigenic minerals.

Early silica diagenesis has been shown to fractionate Si isotopes as a function of the crystallization state, seawater Si concentration, sedimentation rate, and terrigenous mineral content (Tatzel et al., 2015; Geilert et al., 2016). Since the light ^{28}Si isotope is more reactive compared to the heavier isotopes (^{29}Si, ^{30}Si) , processes such as reverse weathering, adsorption, and direct Si~~silica~~ precipitation from saturated solutions show low $\delta^{30}Si$ values in the reaction product and high $\delta^{30}Si$ values in its substrate (i. e. fluids) (e.g. Georg et al., 2006a, 2009; Delstanche et al., 2009; Opfergelt et al., 2013; Geilert et al., 2014; Roerdink et al., 2015; Ehlert et al., 2016). The few modelling and experimental studies, addressing Si isotope fractionation during formation of secondary phases, report isotope fractionation factors between -1.6 and -2‰ (Ziegler et al., 2005; Méheut et al., 2007; Dupuis et al., 2015; Ehlert et al., 2016).

The $\delta^{30}Si$ data for marine pore ~~waters~~ fluids from the Peruvian margin upwelling region, which is characterized by very high diatom productivity and $bSiO_2$-rich sediments (Abrantes et al., 2007; Bruland et al., 2005), agree with these findings and clearly indicate Si isotope fractionation as a consequence of authigenic aluminosilicate precipitation accompanied by a Si isotope fractionation factor of -2.0‰ (Ehlert et al., 2016). Also pore fluids from the Greenland margin and Labrador Sea reflect early diagenetic reactions detected by pore fluid $\delta^{30}Si$ values (between +0.76 and +2.08‰) and the $\delta^{30}Si$ values were interpreted as the product of reverse weathering reactions (Ng et al., 2020). In this study, the Guaymas Basin in the Gulf of California was chosen as study area, as it is characterized by a relatively high diatom productivity and sediments that are predominantly composed of diatomaceous muds (up to 50% diatoms; Kastner and Siever, 1983). Moreover, the Guaymas Basin in the Gulf of California is influenced by hydrothermal activity (e.g. Von Damm, 1990). These $bSiO_2$-rich sediments are thus ideal for dedicated studies of early diagenesis under the influence of different thermal and redox conditions. We investigated the processes controlling Si isotope fractionation during early diagenesis based on pore fluid and $bSiO_2$ data from three fundamentally different environmental settings within the Guaymas Basin including the deep basin, a hydrothermal site, and a site within the Oxygen Minimum Zone (OMZ) on the slope of the Guaymas

Basin (Fig. 1). In addition, the Si isotope composition of the water column, bottom waters, and hydrothermal fluids was determined. A numerical transport-reaction model was applied to the OMZ setting to constrain marine weathering processes and to compare the results to the Peruvian margin. The aim of this study was to constrain the factors controlling Si isotope fractionation during early diagenesis and to identify processes influencing $bSiO_2$ dissolution and authigenic silicate precipitation.

2. GEOLOGICAL SETTING, SAMPLING, AND METHODS

2.1 Geological setting

The Guaymas Basin in the Gulf of California is a currently opening continental rifting environment with two graben systems (northern and southern trough), which are offset by a transform fault and reaches spreading rates of up to 6 cm yr^{-1} (Calvert, 1966). High biological productivity and terrigenous matter input result in high sediment accumulation rates and have produced thick sequences of organic-rich sediments (DeMaster, 1981). Siliceous sediments at the Guaymas Slope show fine laminations within the OMZ (dissolved oxygen <10 µM at ca. 500 – 900 m water depth; Campbell and Gieskes, 1984) due to the absence of burrowing organisms (Calvert, 1964). The Guaymas Basin is characterized by vigorous hydrothermal activity represented by Black Smoker type vents discovered in both the northern and southern troughs (Berndt et al., 2016; Von Damm et al., 1985). Hydrothermal plumes spread horizontally and mix with deep basin water up to 300 m above the seafloor resulting in a fraction of hydrothermal fluids of ~0.1% in the deep waters of the Guaymas Basin (Campbell and Gieskes, 1984). Hydrothermal sills and dikes intruding into the sediments were found to accelerate early diagenetic reactions (due to the released heat) and change pore fluid geochemistry significantly (Gieskes et al., 1982; Kastner and Siever, 1983; Von Damm et al., 1985; Von Damm, 1990). At present, pore fluids in surface sediments show a seawater composition (Geilert et al., 2018) and the absence of diagenetic high-temperature processes render these pore fluids suitable for studying recent early diagenetic processes.

2.2 Sampling

Sediments were sampled via multicorer (MUC) deployment during RV SONNE cruise SO241 in summer 2015 as described in detail in Geilert et al. (2018). In total, 6 stations have been investigated; 4 within the basin (termed basin sites: MUC33-11, MUC22-04, MUC23-05, MUC15-02), one in the vicinity of a hydrothermal vent field (termed hydrothermal site: MUC66-16), and one within the OMZ

(termed OMZ site: MUC29-09) (Fig. 1, Table 1). The coring locations within the basin were sampled in water depths between 1726 and 1855 m below sea level (mbsl). The hydrothermal site (MUC66-16) was sampled in 1842 mbsl and was located at a distance of ~500 m from the active hydrothermal mound described by Berndt et al. (2016). The OMZ site (MUC29-09) was sampled on the Guaymas Basin slope of the Mexican mainland in 665 mbsl.

After core retrieval, bottom water above the sediment was sampled and filtered immediately using 0.2 µm cellulose acetate membrane filters. Bottom water from MUC22-04 may have been contaminated with surface waters during core retrieval as indicated by Si and Mn concentrations (53.8 µM and 0.05 µM, respectively) lower than at the remaining sites within the deep basin, which show distinct anomalies caused by mixing with hydrothermal plume fluids (e.g. MUC15-02: Si = 177.8 µM and Mn = 0.34 µM). Processing of sediments was conducted in a cool laboratory in an argon-flushed glove bag immediately after core retrieval. Sampling intervals were 1-5 cm with the highest resolution close to the sediment surface and increasing distance downcore. Pore fluids were separated from sediments by centrifugation (20 min at 4500 rpm) and subsequently filtered (0.2µm cellulose acetate membrane filters) for further analyses.

Water column samples were taken using a video-guided Niskin Water sampler CTD-Rosette System. Water samples were taken in the basin above MUC15-02 at 1844 mbsl (VCTD02), within the hydrothermal plume between 1781 and 1800 mbsl (VCTD06 and 09) above the Black Smoker mound as described in Berndt et al. (2016), and above the OMZ site (MUC29-09) at 586 mbsl (Fig. 1).

2.3 $bSiO_2$ separation and digestion

The $bSiO_2$ mass fractions of sediment samples were determined using an automated leaching method following Müller and Schneider (1993) at GEOMAR Helmholtz-Centre for Ocean Research Kiel. The sample material was treated with 1M NaOH at 85°C to extract the opal fraction. The increase in dissolved Si~~silica~~ was monitored and evaluated using a method described by DeMaster (1981). The precision of the mass fraction determination was 5 to 10% (1SD). The $bSiO_2$ was separated from the sediment for Si isotope analyses following the method of Morley et al. (2004). About 500 mg of a freeze-dried sediment sample was transferred into a centrifuge tube. Organic matter and carbonate material was removed by adding H_2O_2 (Suprapur) and HCl, respectively. Clay particles (grain size <2µm) were separated from the remaining sediment by the Atterberg method following Stoke's law (Müller, 1967). The remaining sediment ($bSiO_2$ and heavy minerals) was sieved using a 5 µm-sieve and subsequently separated from the remaining detritus using heavy liquid separation (sodium-polytungstate solution). The heavy liquid purification method was repeated until

clean, examined via light microscopy, $bSiO_2$ samples (>95%) were obtained. Light microscopy revealed that the $bSiO_2$ fraction essentially consisted of diatoms and only traces of radiolarians and sponges were present (<5%). The $bSiO_2$ samples were stored in Milli-Q water (MQ water). The $bSiO_2$ sample of the OMZ site stems from a nearby gravity core (GC07), which is described in detail in Geilert et al. (2018). The $bSiO_2$ samples were dissolved following a method by (Reynolds et al., (2008). Aliquots of the cleaned $bSiO_2$ samples were transferred into Teflon vials and dried on a hot plate. Drying of the samples was shown by (Ehlert et al., (2012) to have no effect the Si isotope composition of the samples. Subsequently, 1 ml of 0.1 M NaOH was added and the samples were placed on a hot plate at 130°C for 24 hours. After sample digestion, the supernatant and residue (undissolved traces of radiolarians and sponges) were separated via centrifugation. The supernatant was treated with 200 µl H_2O_2 (Suprapur) in order to remove remaining organic matter and then dried and re-dissolved in 1 ml 0.1 M NaOH at 130°C for 24 hours. After the digestion procedure, the samples were diluted with MQ water and neutralized with 1 M HCl.

2.4 XRD measurements

X-ray diffraction analyses of the dried clay samples were performed at the Central Laboratory for Crystallography and Applied Material Science, ZEKAM, dept. of Geosciences, University Bremen, using a Philips X'Pert Pro multipurpose diffractometer. The diffractometer was equipped with a Cu-tube, a fixed divergent slit of $\frac{1}{4}°$, a secondary Ni filter, and a X'Celerator detector system. A continuous scan from 3 to 85° 2θ was applied for the measurements with a calculated step size of 0.016° 2θ (calculated time per step was 50 seconds). Quantification of mineral phases were based on the Philips software X'Pert High Score™, the freely available X-ray diffraction software MacDiff 4.25 (Petschick et al., 1996), and the QUAX full-pattern method after Vogt et al. (2002). The standard deviation is ±1-3% for well crystallized minerals (see also Vogt et al., 2002) and ±5% for the remaining mineral phases.

2.5 Geochemical analyses of fluid and solid phases

Analyses of major and trace element concentrations of pore fluids from the basin sites and the hydrothermal site as well as the water column are described in Geilert et al. (2018). OMZ site pore fluids were treated in the same way. In brief, the pore fluids were analysed onboard by photometry (NH_4) and on shore for dissolved anions (Cl) and cations (Si, K, Na, Mg) using ion chromatography (IC, METROHM 761 Compact, conductivity mode) and inductively coupled plasma optical emission spectrometry (ICP-OES, VARIAN 720-ES), respectively. Analytical precision was constrained using the

IAPSO seawater standard for all chemical analyses (Gieskes et al., 1991) and was found to be <1% for Cl, <2% for K, Na, Mg, and <5% for Si.

Freeze dried and ground sediment samples were digested in HF (40% Suprapur), HNO_3 (Suprapur), and $HClO_4$ (60% p.a.) for major element analyses. The accuracy of the method was tested by method blanks and the reference standards SDO-1 (Devonian Ohio Shale, USGS) and MESS-3 (Marine Sediment Reference Material, Canadian Research Council). The digested samples were measured for their K and Al contents by ICP-OES (VARIAN 720-ES) and reproducibility was ≤5%. Total carbon (TC) and total organic carbon (TOC) were measured in freeze-dried and ground sediment samples by flash combustion using the Carlo Erba Element Analyzer (NA-1500). Carbonate carbon ($CaCO_3$) was calculated by subtracting TOC from TC.

The digested $bSiO_2$ samples were analyzed for their Al and Si contents using the Agilent 7500 series quadrupole ICPMS at GEOMAR to provide information about potential clay contamination of the separated $bSiO_2$ fraction (Shemesh et al., 1988), whereby Al/Si ratios below 50 mM/M are considered as negligible clay contamination (van Bennekom et al., 1988; Hurd, 1973). Al/Si ratios in the studied $bSiO_2$ ranged between 15 and 39 mM/M, with three exceptions in MUC22-04, MUC15-02, and MUC66-16 yielding Al/Si ratios of 71 mM/M, 57 mM/M, 50 mM/M, respectively. However, all $\delta^{30}Si_{bSiO2}$ values agreed well with surrounding $\delta^{30}Si_{bSiO2}$ values and clay contamination is thus considered ~~insignificant~~unimportant. All other $bSiO_2$ samples are considered clay-free.

2.6 Sample purification and Si isotope measurements

Fluid and digested $bSiO_2$ samples were prepared for Si isotope measurements following the purification method of Georg et al. (2006b). The concentration of the samples was adjusted and loaded (1 ml with ~64 µM Si) onto 1 ml pre-cleaned cation-exchange resin (Biorad AG50 W-X8) and subsequently eluted with 2 ml MQ water. Matrix effects originating from dissolved organic compounds and anions, which cannot be separated by this purification method, have previously been found to potentially influence Si isotope measurements (van den Boorn et al., 2009; Hughes et al., 2011). However, no influence of the matrix effects on pore fluid Si isotope measurements has been found during our measurements following several tests described in Ehlert et al. (2016). Briefly, Ehlert et al. (2016) removed organic compounds by H_2O_2 and ~~and~~ SO_4 by Ba addition yielding $\delta^{30}Si$ values identical to untreated samples, within error. Therefore, our samples were not treated with H_2O_2 or Ba before sample purification and Si isotope measurements.

Si isotope samples were measured in medium resolution on a NuPlasma MC-ICPMS (Nu InstrumentsTM, Wrexham, UK) at GEOMAR using the Cetac Aridus II desolvator. Sample Si concentrations of about 21 µM resulted in a ^{28}Si intensity of 3 to 4 V. The MQ blank was ≤ 3mV, resulting in a blank to signal ratio <0.1 %. The measurements were performed using the standard-sample bracketing method to account for mass bias drifts of the instrument (Albarède et al., 2004). Si isotopes are reported in the $\delta^{30}Si$ notation, representing the deviation of the sample $^{30}Si/^{28}Si$ from that of the international Si standard NBS28 in permil (‰). Long-term $\delta^{30}Si$ values of the reference materials Big Batch (-10.6±0.2‰; 2SD; n=49), IRMM018 (-1.5±0.2‰; 2SD; n=48), Diatomite (+1.3±0.2‰; 2SD; n=44), and BHVO-2 (-0.3±0.2‰; 2SD; n=13) are in good agreement with $\delta^{30}Si$ values in the literature (e.g. Reynolds et al., 2007; Zambardi and Poitrasson, 2011). The seawater inter-calibration standard Aloha (1000 m) resulted in +1.3±0.2‰ (2SD; n=8) in very good agreement to Grasse et al. (2017). Additionally, two in-house matrix standards have been measured. The pore fluid matrix standard yielded an average $\delta^{30}Si$ value of +1.3±0.2‰ (2SD; n=17) and the diatom matrix standard (E. rex) -1.0±0.2‰ (2SD; n=22), which agrees well with earlier reported values (Ehlert et al., 2016). All samples were measured 2-4 times on different days and the resulting $\delta^{30}Si$ values have uncertainties between 0.1 and 0.4‰ (2SD, Table 1). The $\delta^{30}Si$ values of pore fluids, $bSiO_2$, and bottom water are given as $\delta^{30}Si_{pf}$, $\delta^{30}Si_{bSiO2}$, and $\delta^{30}Si_{bw}$, respectively. Error bars in the figures indicate the uncertainty of the individual sample measurements (two standard deviation, 2SD).

2.7 Numerical model

A numerical reactive-transport model was applied to simulate Si turnover within OMZ site sediments. The model was based on a previously published Si isotope model (Ehlert et al., 2016) and was extended to consider the dissolution of additional phases. A detailed description of the model can be found in the supplementary information.

2.8 Calculation of the amount of terrigenous material and mass accumulation rate

The amount of terrigenous material (%) for the Guaymas Basin was calculated as the total mass subtracted by the carbonate content ($CaCO_3$), the organic matter content (OC), and the $bSiO_2$ content (Sayles et al., 2001):

$$\text{Terrigenous material} = 100 - (CaCO_3 + OC + bSiO_2) \quad (1)$$

The mass accumulation rate (MAR) was calculated as

$$MAR = S^{*}d^{*}(1- \Phi) \quad (2)$$

with S the sedimentation rate as 0.18 cm yr^{-1} (Thunell et al., 1994) and d the bulk dry density as 2.5 g cm^{-3}. The porosity (Φ) was taken at the deepest part of the core with 0.925.

3. RESULTS

3.1 Water chemistry and sediment composition

All water column, pore fluid, and hydrothermal Si concentration data, $bSiO_2$ weight fractions as well as Si isotope values are reported in Tables 1 and 2. A detailed description of the water column properties, pore fluids, and hydrothermal fluid chemistry can be found in Berndt et al. (2016) and Geilert et al. (2018). Pore fluids predominantly show a seawater composition at all sampling sites and are not influenced by high temperature processes related to sill intrusions or mixing with hydrothermal fluids. Pore fluid geochemistry of major elements in the OMZ resembles that of the remaining sampling sites with the exception of a strong enrichment in NH_4 (Table ~~1S~~ S1 and Geilert et al., 2018) as well as high Fe and low Mn concentrations (Scholz et al., 2019). The porosity corrected K (see supplement) and Al contents in the sediments ranged between 0.9 and 21.2 wt% and 2.9 and 66.6 wt%, respectively (Table 1). The TOC contents ranged between 0.3 and 7.8 % and are shown in Table ~~1S~~S1.

3.2 Bottom water, water column, and hydrothermal fluid Si concentrations and $\delta^{30}Si$ values

The bottom water Si concentration ranged between 173 and 254 µM for all basin sites and the hydrothermal site (between 1726 and 1855 mbsl) with the exception of MUC22-04, where Si concentrations were as low as 54 µM (possible surface water contamination, see section 2.2 and Table 1). The bottom water $\delta^{30}Si_{bw}$ signatures ranged between +1.5‰ and +2.0‰ for all basin sites and the hydrothermal site and overlap within error (average $\delta^{30}Si_{bw}$: +1.8±0.2‰, 1SD; highest $\delta^{30}Si_{bw}$ for surface contaminated sample (MUC22-04)). Bottom water Si concentration for the OMZ site was 31 µM (665m water depth). The bottom water within the OMZ site had a distinctly lower $\delta^{30}Si_{bw}$ value of +0.8‰. Here, a potential contamination with surface waters can be excluded given that they are characterized by high $\delta^{30}Si$ values (from 1.7 to 4.4‰; Ehlert et al., 2012; Grasse et al., 2013), due to the preferential biological uptake of ^{28}Si (~~de~~ De ~~la~~ La Rocha et al., 1997).

The basin water (VCTD02), which was sampled about 1 m above the seafloor, had a Si concentration of 163 µM and a $\delta^{30}Si_{deepBasin}$ value of +1.5‰. Hydrothermal plume Si concentrations ranged between 253 and 690 µM and $\delta^{30}Si$ values ranged from +0.7‰ (VCTD09-06) to +1.4‰ (VCTD06-06). The water column within the OMZ (586 mbsl) had a Si concentration of 78 µM and a $\delta^{30}Si_{OMZ}$ value of +1.5‰ (Table 2).

3.3 Pore fluid Si concentration and $\delta^{30}Si_{pf}$ values

Pore fluid Si concentrations generally increased asymptotically with depth from bottom water values until reaching maximum average concentrations between 605 and 864 µM Si (Table 1, Fig. 2). For the basin sites MUC33-11 and MUC15-02 as well as the OMZ site the Si concentrations asymptotically increased until average values of 742 (≥8 cm below seafloor (cmbsf)), 729 (≥9 cmbsf), and 765 (≥9 cmbsf) µM were reached, respectively. Hydrothermal site Si concentrations were higher and increased to 864 µM (≥4.5 cmbsf). MUC22-04 and MUC23-05 Si concentrations initially increased to values of on average 605 µM (5.5 - 11 cmbsf) and 735 µM (3.5 - 9 cmbsf) and then decreased again to 364 µM (26 cmbsf) and 640 µM (22 cmbsf), respectively.

Pore fluid $\delta^{30}Si_{pf}$ values for all basin sites ranged from +0.9‰ to +1.5‰ (Table 1, Fig. 2), which is lower than the respective bottom water $\delta^{30}Si_{BW}$ values ($\delta^{30}Si_{BW}$ from +1.6‰ to +2.0‰). The decrease in Si concentration at MUC22-04 and MUC23-05 below 13 cmbsf and 11 cm cmbsf, respectively, is not reflected in a significant change in $\delta^{30}Si_{pf}$. The hydrothermal site showed the highest $\delta^{30}Si_{pf}$ values ranging from +1.8‰ and +2.2‰, which is higher than the bottom water $\delta^{30}Si_{BW}$ (+1.5‰). In contrast, the OMZ site had the lowest $\delta^{30}Si_{pf}$ values between -0.5‰ and +0.8‰, which was also characterized by very low $\delta^{30}Si_{bw}$ (+0.8‰; Table 1).

3.4 $bSiO_2$ content and $\delta^{30}Si_{bSiO2}$ values

The $bSiO_2$ content of the sediments (Table 1, Fig. 2) varied between 4.7 wt% and 47.6 wt%. Lowest contents were present at the basin site MUC22-04 (7.6 -13.1 wt%) and the hydrothermal site (4.7 - 14.6 wt%). The remaining sampling sites showed higher $bSiO_2$ contents of on average 23±7 wt% (1SD). The $\delta^{30}Si_{bSiO2}$ signatures ranged between +0.4‰ and +1.0‰ and did not vary systematically with depth or sampling site within error. The small variability in $\delta^{30}Si_{bSiO2}$ signatures most likely stems from natural variability within the Guaymas Basin.

3.5 XRD results of the clay fraction

The main silicate mineral phases of all samples were phyllosilicates (16-59 wt%), primary silicates (quartz, plagioclase, potassium feldspar; 15-38 wt%), and amorphous SiO_2 (4-43 wt% including abiogenic and biogenic opal) (Table ~~2S~~S2). The phyllosilicates were mainly composed of variable fractions of smectite, illite, montmorillonite, and kaolinite. Apart from silicate minerals, minor amounts of Fe-(hydr-)oxides (≤10 wt%, most between 2 and 3 wt%), pyroxenes (≤8 wt%), and carbonates (≤6 wt%) were present. Biogenic opal fragments were identified via light microscopy to be the dominating amorphous silicate phase at all sites besides the hydrothermal site and MUC23-05 in the basin basin. At the hydrothermal site, the abiogenic amorphous silica fraction was the dominating silica phase in the uppermost and lowermost core sections with only minor occurrences of biogenic opal fragments. Abiogenic amorphous silica was also found in the uppermost and lowermost core sections of MUC23-05.

4. DISCUSSION

Pore fluid Si concentration and $\delta^{30}Si_{pf}$ signatures vary significantly between sampling sites and appear to depend strongly on ambient conditions. The Si concentration and isotope compositions are proposed to be affected by dissolution of $bSiO_2$, the dissolution of terrigenous phases, and the formation of authigenic aluminosilicates; the latter process is defined as reverse weathering. Dissolution of $bSiO_2$ is most effective in the reactive surface layer (≤ 10 cmbsf) where the degree of Si~~silica~~ undersaturation is highest. ~~As soon as~~When Si is released into solution via $bSiO_2$ dissolution, certain amounts of Si re-precipitate~~s~~ as authigenic aluminosilicates as a function of the availability of reactive metals, made available by dissolution of terrigenous material (e.g. Michalopoulos and Aller, 1995; Van Cappellen and Qiu, 1997a,b; Loucaides et al., 2010). In the course of this process authigenic silicate precipitation induces $\delta^{30}Si$ fractionation, whereby the ^{28}Si is preferentially incorporated into the solid phase, enriching the remaining fluid in ^{30}Si (~~e.g. Georg et al., 2006a; Opfergelt et al., 2013;~~ Ehlert et al., 2016). In the following sections, the processes during early diagenesis influencing pore fluid $\delta^{30}Si_{pf}$ signatures under different ambient conditions are discussed. For the OMZ site, we quantify these processes using a reactive transport model and compare the results to the only other OMZ site where pore fluid $\delta^{30}Si_{pf}$ data is available, the Peruvian margin.

4.1. Influences on $\delta^{30}Si_{pf}$ due to source mixing

In the open ocean, a strong correlation between the inverse Si concentration (1/Si) and Si isotope composition in intermediate and deep waters exists, showing low $\delta^{30}Si$ values with high Si

concentrations and can be used to identify water mass mixing between two endmembers with distinct Si characteristics (e.g. de Souza et al., 2012). Here, we use the two endmember mixing Eq. (3) to calculate the mixing between the deep water column and fluids originating from $bSiO_2$ dissolution according to

$$\delta^{30}Si_{mix} = \frac{(\delta^{30}Si_{\text{water column}} * [Si]_{\text{water column}} * f) + (\delta^{30}Si_{bSiO2} * [Si]_{bSiO2} * (1-f))}{([Si]_{\text{water column}} * f) + ([Si]_{bSiO2} * (1-f))} \quad (3)$$

with $\delta^{30}Si_{\text{water column}}$ and $[Si]_{\text{water column}}$ as the respective water column Si isotope composition and concentration (Table 2) and $\delta^{30}Si_{bSiO2}$ as the average $bSiO_2$ value (+0.8‰) of all sites. The equilibrium concentration in respect to $bSiO_2$ dissolution was derived from an experimental study by Van Cappellen and Qiu (1997a) with $[Si]_{bSiO2}$ = 900µM. Mixing fractions are represented by *f*, varied over 100% water column and 0% fluids affected by $bSiO_2$ dissolution and vice versa.

Pore fluid $\delta^{30}Si_{pf}$ values of all sites deviate from mixing curves between the deep water column and fluids originating from $bSiO_2$ dissolution and are obviously affected by additional processes (Fig. 3). Si isotope fractionation during $bSiO_2$ dissolution is not well constrained and ranges between -0.55‰ and 0‰, while most studies argue against a significant isotope effect (Demarest et al., 2009; Egan et al., 2012; Wetzel et al., 2014). Therefore, we will also exclude Si isotope fractionation in dependence of $bSiO_2$ dissolution as a process affecting pore fluid $\delta^{30}Si_{pf}$ values. The $\delta^{30}Si_{pf}$ values of the basin sites and hydrothermal site are higher (+0.9‰ to +2.2‰) compared to the respective mixing curves, while $\delta^{30}Si_{pf}$ values of the OMZ site are lower (-0.5‰ to +0.8‰). While a shift to lower $\delta^{30}Si_{pf}$ values ~~compared to fluid mixing~~ points to dissolution of an isotopically light phase, ~~show~~ higher $\delta^{30}Si_{pf}$ values indicate that precipitation processes are important, given that the light Si isotope is preferentially incorporated in authigenic secondary phases (Georg et al., 2009). This indicates that processes governing the pore fluid Si isotope composition differ significantly between the individual sites.

4.2. Influences on $\delta^{30}Si_{pf}$ from terrigenous and biogenic material

The terrigenous/$bSiO_2$ ratio was found to be the main mechanism controlling asymptotic pore fluid Si concentration and the benthic Si flux (Van Cappellen and Qiu, 1997a, b). Maximum Si concentrations were reached asymptotically at four out of six sampling sites (Fig. 2). Two sites within the basin (MUC22-04 and MUC23-05) show lower Si concentrations in the deep core sections (Fig. 2), which are most likely related to the decrease of reactive silica with depth, caused by the formation of less soluble silica phases (Van Cappellen and Qiu, 1997a). At these sites, the asymptotic Si concentration

is defined as the maximum concentration values in the center of the core. The amount of terrigenous material for the Guaymas Basin was calculated according to Eq. (1) and accounts for 75%.

Asymptotic Si concentrations plotted against the terrigenous/$bSiO_2$ ratio fall on the global trend except for the hydrothermal site (Fig. 4a). Here, high geothermal gradients are likely responsible for the higher Si concentrations with respect to the global trend (see also section 4.3.2). In contrast to the asymptotic Si concentration, no strong correlation of the pore fluid $\delta^{30}Si_{pf}$ values with the terrigenous/$bSiO_2$ ratio exists (Fig. 4b). In order to identify processes responsible for the different pore fluid $\delta^{30}Si_{pf}$ values and to facilitate comparison between the three settings within the Guaymas Basin, only average $\delta^{30}Si_{pf}$ values will be discussed in the following.

Average $\delta^{30}Si_{pf}$ values show distinct variations between the individual settings. The $\delta^{30}Si_{pf}$ values of the OMZ site are lower (0.0±0.5‰, 1SD, n = 6) than those of the basin sites (+1.2±0.1‰, 1SD, n = 17) and the hydrothermal site, which shows the highest $\delta^{30}Si_{pf}$ values (+2.0±0.2‰, 1SD, n = 3). The homogeneity of the individual $\delta^{30}Si_{pf}$ profiles indicates that possible effects of bioirrigation at the basin sites and hydrothermal site are quickly compensated by isotopic exchange. Similarly, bioturbation has also little impact on the sediment composition given the the homogeneity of the $bSiO_2$ content profiles with depth (Fig. 2).

4.3 Influence of the ambient environmental conditions on the $\delta^{30}Si_{pf}$ values

4.3.1 Basin sites

Pore fluid $\delta^{30}Si_{pf}$ values of the basin sites deviate from the mixing curve between the deep water column and fluids originating from $bSiO_2$ dissolution and are shifted to higher values (+1.2±0.1‰; Fig. 3). This shift to higher $\delta^{30}Si_{pf}$ values can be explained by Si re-precipitation as authigenic aluminosilicates, which preferentially incorporate the light ^{28}Si isotope (Fig. 5a). Alteration of terrigenous material leads to mobilization and re-precipitation of Al and the uptake of K from seawater in the authigenic phase (Michalopoulos and Aller, 2004). The sedimentary K/Al ratio can thus be used to detect these early diagenetic reactions in addition to pore fluid $\delta^{30}Si_{pf}$ values. Authigenic aluminosilicates formed during alteration of terrigenous material were found to have K/Al ratios of 0.32 (Michalopoulos and Aller, 2004), which is higher than the pristine K/Al ratio of terrigenous material carried by rivers (K/Al = 0.19; Viers et al., 2009). The average K/Al ratio of the basin sites is 0.34±0.01 (1SD), which is in the same range as K/Al ratios – indicative of authigenic aluminosilicate formation (Michalopoulos and Aller, 2004). ~~Thus, $bSiO_2$ dissolution and re-~~

~~precipitation of Si in authigenic aluminosilicates control the pore fluid $\delta^{30}Si_{pf}$ values in the basin sites.~~ Thus, at basin sites both K/Al ratios and $\delta^{30}Si_{pf}$ values are in agreement to recognize $bSiO_2$ dissolution followed by authigenic clay formation as significant processes taking place.

4.3.2 Hydrothermal site

The $\delta^{30}Si_{pf}$ values from the hydrothermal site are higher (+2.0±0.2‰) than the mixing curve between the deep water column and fluids originating from $bSiO_2$ dissolution and also much higher than pore fluid $\delta^{30}Si_{pf}$ values from the basin (Fig. 3, 5a). The high $\delta^{30}Si_{pf}$ values indicate that precipitation plays a significant role at this site. Sedimentary K/Al ratios are equivalent to basin values (K/Al = 0.34) and thus show the formation of authigenic aluminosilicates. Consequently, the higher pore fluid $\delta^{30}Si_{pf}$ values compared to the basin sites can either be explained by a different Si isotope fractionation factor or by the precipitation of additional silica phases. The hydrothermal site is located in close proximity to a hydrothermal vent field and hydrothermal deposits are mainly composed of Fe-sulfides (Berndt et al., 2016), while nearby sediments are dominated by amorphous silica, quartz, and Fe-Si silicates (e.g. ferrosilite, fayalite) (Kastner, 1982; Von Damm et al., 1985). Si adsorption to iron (oxyhydr)oxide and incorporation into Fe-Si gels can create substantial Si isotope fractionation with ^{28}Si being preferentially enriched in the solid phase (Delstanche et al., 2009; Zheng et al., 2016). Pore fluids show high Fe^{2+} concentrations (up to 190 µM; Scholz et al., 2019) and the precipitation of Fe-Si silicates is thus likely, shifting pore fluid $\delta^{30}Si_{pf}$ to the observed high values. Saturation indices calculated based on the program PHREEQC (Parkhurst and Appelo, 1999) indicate that quartz is supersaturated and amorphous silica is close to saturation at about > 6cmbsf (Fig. S1). Due to the dynamics of hydrothermal systems, this can be subject to changes and supersaturation of amorphous silica is likely to be obtained occasionally, due to the ascent of Si enriched fluids from greater depth. ~~Si concentrations lower than amorphous Si and quartz solubilities at various depths (this study; Von Damm et al., 1985; Gieskes et al., 1988), indicating precipitation of the respective mineral phase during pore fluid ascent.~~ Gieskes et al. (1988) reported on amorphous silica cement in the hydrothermally-influenced sediments of the Guaymas Basin, which is supported by findings of this study and likely explains the high amorphous SiO_2 contents identified by XRD (~35 wt%; see Sect. 3.5; Table ~~2S~~S2). In the Guaymas Basin, high thermal gradients (up to 11 K m^{-1}; Geilert et al., 2018) caused by igneous sill intrusions near the active spreading center significantly influence diagenetic reactions at depth and accelerate Si dissolution and precipitation (Fig. 5a) (e.g. Kastner and Siever, 1983). This can also explain the high pore fluid $\delta^{30}Si_{pf}$ values, given that deep Si saturated fluids ascent and Si precipitates, likely along with Fe, over a large temperature range, whereby lower temperatures are

485 associated with larger Si isotope fractionation shifting pore fluid $\delta^{30}Si_{pf}$ to the observed high values
486 (Geilert et al., 2014; Zheng et al., 2016).
487
488 4.3.3 OMZ site
489
490 At the OMZ site, the $\delta^{30}Si_{pf}$ values are significantly lower (on average 0.0±0.5‰) than the water
491 column $\delta^{30}Si_{water\ column}$ value (+1.5±0.2‰) and also lower than the $\delta^{30}Si_{bSiO2}$ value (+0.8‰) (Fig. 2, 3).
492 Interestingly, the only other $\delta^{30}Si_{pf}$ values from an OMZ were obtained at the Peruvian margin (Ehlert
493 et al., 2016), where the $\delta^{30}Si_{pf}$ values in the upper 10 cmbsf are slightly higher than the water column
494 $\delta^{30}Si_{bw}$ values (+1.~~6~~8‰ and +1.5‰, respectively). As Ehlert et al. (2016) concluded, the Peruvian
495 $\delta^{30}Si_{pf}$ values are influenced by $bSiO_2$ dissolution and precipitation of authigenic aluminosilicates, the
496 latter process shifting pore fluid $\delta^{30}Si_{pf}$ to values higher than those of the water column.
497 Consequently, in order to explain the extremely low $\delta^{30}Si_{pf}$ values at the Guaymas Basin OMZ, an
498 additional process must occur. We hypothesize that a phase enriched in ^{28}Si needs to dissolve in
499 order to shift the pore fluid $\delta^{30}Si_{pf}$ values and this phase might be 1) iron (oxyhydr)oxides with
500 adsorbed ^{28}Si or 2) terrestrial clays.
501
502 Silicon exhibits a strong affinity to iron (oxyhydr)oxides (see also section 4.3.2; Davis et al., 2002) and
503 Si isotopes fractionate significantly during Si adsorption and co-precipitation (Delstanche et al., 2009;
504 Zheng et al., 2016). Dissolved Fe^{2+} in pore fluids can be transferred across the sediment-water
505 interface via diffusion and re-precipitates as iron (oxyhydr)oxides, where it subsequently dissolves
506 again in the reducing sediment. This process can repeat, resulting in multiple cycles of Fe dissolution
507 and re-precipitation on the Guaymas Basin slope (Scholz et al., 2019). We hypothesize that the light
508 ^{28}Si adsorbs to iron (oxyhydr)oxides in the water column and that upon reductive dissolution of Fe
509 minerals in the surface sediment, the light ^{28}Si isotope is re-released into the pore fluids, adding to
510 the observed low $\delta^{30}Si_{pf}$ values. However, the quantification of this Fe-Si shuttle and the contribution
511 to the low $\delta^{30}Si_{pf}$ values ~~to the~~in OMZ pore fluids remains difficult given that Fe undergoes multiple
512 cycles of dissolution and re-precipitation. Furthermore, the exact process of complexation, Si isotope
513 fractionation, and co-precipitation is unknown and requires further investigations (see also Fig. S3).
514 We can only speculate that the transport of ^{28}Si via the Fe-Si shuttle is only of minor importance
515 given that the MAR of $bSiO_2$ and terrigenous material are dominating the Si supply to Guaymas OMZ
516 sediments (Calvert, 1966; DeMaster, 1981).
517
518 The low $\delta^{30}Si_{pf}$ values can also be explained by dissolution of terrigenous clay particles, which are
519 generally enriched in ^{28}Si, showing a large range in $\delta^{30}Si$ with the majority between -3‰ to 0‰

(Frings et al., 2016 and references therein). Primary minerals like feldspars or olivine, which are generally considered to control marine weathering reactions (e.g. Wallmann et al., 2008) have higher $\delta^{30}Si$ values (e.g. feldspars with -0.15‰; Georg et al., 2009) and their dissolution alone cannot create the low pore fluid $\delta^{30}Si_{pf}$ values (see supplement and Fig. S6). Clays are usually considered to be the stable end product of silicate weathering. However, fine clay particles and highly reactive surface sites of clays such as montmorillonite, smectite and illite may dissolve in natural waters (Cappelli et al., 2018; Golubev et al., 2006; Köhler et al., 2005). The dissolution is promoted by organic ligands and the reduction of structural iron of clay minerals under reducing conditions (Anderson and Raiswell, 2004). Humic substances that are abundant in OMZ sediments enriched in organic matter may catalyze the microbial reduction of structural iron in clays (Lovley et al., 1998) and their dissolution (Liu et al., 2017). Clays are abundant in OMZ sediments, given that fine-grained terrigenous material is transported downslope from the shelf to the basin (Scholz et al., 2019). Furthermore, the microbial oxidation of ferrous Fe in these fine-grained silicate minerals and its subsequent conversion to reactive iron minerals was also found to contribute to the Fe cycling at the Guaymas Basin slope (Scholz et al., 2019).

In order to constrain the possibility of terrigenous clay dissolution and the related shift to low $\delta^{30}Si_{pf}$ values in the Guaymas OMZ a reactive transport model was applied, based on our previously published $\delta^{30}Si$ model (Ehlert et al., 2016). The data obtained at the Guaymas OMZ were used to model the turnover of Si in these sediments and the previously published model extended to consider additional processes (Fig. 6). A full description of the model is presented in the supplementary information. The model was fit to dissolved Si~~silica~~ concentrations and $\delta^{30}Si$ values measured in pore fluids and biogenic opal and K/Al ratios determined in the solid phase (Fig. 6). High rates of terrigenous clay dissolution were applied at the sediment surface to reproduce the observed minima in $\delta^{30}Si_{pf}$ pore fluid values and K/Al ratios in a model run best fitting our data set (Fig. 6, best fit). Since the terrigenous phases deposited at the sediment surface contain potassium (K_{terr} = 1.7 wt%, K/Al = 0.19; Viers et al., 2009) and are depleted in ^{30}Si (clay $\delta^{30}Si$ (late stage weathering product) = -2‰; Opfergelt et al., 2010)(~~clay $\delta^{30}Si \approx -2‰$; Frings et al., 2016 and references therein~~), the dissolution of these phases induces a decline in pore fluid $\delta^{30}Si$ and solid phase K/Al (supplementary information). The precipitation of authigenic phases that are depleted in ^{30}Si (Si isotop~~p~~e fractionation: $\Delta^{30}Si_{au}$ = -2‰; Ehlert et al., 2016) and characterized by high K contents (K/Al = 0.32; Michalopoulos and Aller, 2004) induces a down-core increase in pore fluid $\delta^{30}Si_{pf}$ and solid phase K/Al below the surface minimum. Consequently, terrigenous clay dissolution under the reducing conditions of the OMZ and subsequent authigenic aluminosilicate precipitation can explain the low $\delta^{30}Si_{pf}$ values detected in Guaymas OMZ pore fluids (Fig. 5). However, our model results should be

regarded with caution because we applied strongly simplifying assumptions (e.g. steady state, simple rate laws). Moreover, our estimates of solid phase reactivity and isotopic composition are preliminary and not supported by independent data.

Additional simulations were conducted to investigate how the solid phase and pore fluid composition is affected by the dissolution of terrigenous clay phases and the precipitation of authigenic phases (Fig. 6) and how varying $\delta^{30}Si$ values of the dissolving terrigenous phase and Si isotope fractionation factors impact pore fluid $\delta^{30}Si_{pf}$ values (Fig. S6). Furthermore, varying K/Al ratios and $bSiO_2$ solubilities are tested (see supplement). The surface minima in pore fluid $\delta^{30}Si_{pf}$ and solid phase K/Al disappear when the dissolution rate is set to zero ($R_{terr} = 0$) while the ongoing precipitation of authigenic phases leads to a strong down-core increase and high values at depth that are not consistent with the data. Pore fluid $\delta^{30}Si_{pf}$ and solid phase K/Al values strongly decrease with depth when the rate of authigenic phase precipitation is set to zero ($R_{au} = 0$) such that the model yields values that are significantly lower than the measured values. Dissolved Si~~silica~~ concentrations cannot be used to further constrain R_{terr} and R_{au} because they are largely controlled by the dissolution of biogenic opal (R_{opal}). Dissolved K concentrations show a much lower sensitivity to R_{terr} and R_{au} than solid phase K/Al ratios due to the high porosity of the OMZ sediments. Changes in dissolved K are largely eliminated by molecular diffusion that is favored by the high porosity while the effect of the solid phase reactions R_{terr} and R_{au} on the pore fluid composition is diminished by the low solid phase contents and the high background concentration of dissolved K in ambient bottom waters. However, the model runs show that the more sensitive pore fluid $\delta^{30}Si_{pf}$ and solid phase K/Al can be used to constrain the balance between the dissolution of terrigenous phases and the precipitation of authigenic phases and that both reactions are required to model the low $\delta^{30}Si_{pf}$ values measured in the Guaymas OMZ. Additionally, $\delta^{30}Si$ values for the dissolving terrigenous material higher than -2‰ cannot reproduce the measured $\delta^{30}Si$ values in the OMZ pore fluids. Only if the fractionation factor is lowered to -1‰, terrigenous material with $\delta^{30}Si$ values of -1.7‰ can produce the observed values (Fig. S6). Thus, low pore fluid $\delta^{30}Si$ values in the Guaymas OMZ can only be reproduced by dissolving terrigenous clay particles highly depleted in ^{30}Si.

The modelled Si isotope composition of the benthic flux is -0.97‰, which is lower than the $\delta^{30}Si$ value of the bottom water (+0.8‰). The higher bottom water $\delta^{30}Si$ value along with the low Si concentration (~30µM), which is lower than the ambient water column Si concentration (~80µM), indicates that a certain amount of Si must directly re-precipitate at the sediment water interface. Still the $\delta^{30}Si$ of the bottom water is lower compared to the ambient water column, showing a benthic Si flux with low $\delta^{30}Si$ values at continental margin settings, which is also in excellent agreement with

previously modelled and calculated $\delta^{30}Si$ values (Ehlert et al., 2016; Grasse et al., 2016). These findings show that benthic Si fluxes at continental margins are a source of low $\delta^{30}Si$ values to the ocean and need to be taken into account in future marine Si budget models.

4.4 Controlling processes and the impact on the global marine Si cycle

Stable and radioactive Si isotope data revealed significant sedimentary import and export processes influencing the marine Si~~silica~~ cycle (Ehlert et al., 2013, 2016; Tréguer and De La Rocha, 2013; Grasse et al., 2016; Rahman et al., 2017; Sutton et al., 2018). Diatom burial removes about 9.9 Tmol yr^{-1} Si from the ocean to the sediments, however, effects of terrigenous silicate dissolution and reverse silicate weathering on $bSiO_2$ burial, preservation, and the benthic Si flux (and its Si isotope composition) are not well constrained (Sutton et al., 2018). It has previously been shown that silicate minerals dissolve in deep methanogenic sediments where the dissolution process is favored by high CO_2 and organic ligand concentrations in ambient pore fluids (Wallmann et al., 2008). Similar to chemical weathering on land, the dissolution of terrigenous silicate phases in marine sediments leads to a release of cations and the conversion of CO_2 into HCO_3^-. Moreover, this marine weathering process provides the dissolved Al that is needed for reverse weathering reactions. Our OMZ data show for the first time that marine silicate weathering (dissolution of terrigenous silicates) also occurs in OMZ surface sediments where it can outpace reverse weathering (precipitation of authigenic silicates). Our study indicates that ambient environmental conditions appear to significantly influence the balance between marine weathering and reverse weathering and thereby the Si flux back to the ocean. Pore fluid $\delta^{30}Si_{pf}$ values depend on a complex interplay between $bSiO_2$, terrigenous silicate dissolution, and authigenic aluminosilicate precipitation, however, the controlling factors that determine which process dominates are difficult to constrain (Fig. 5). In view of the OMZ settings (Guaymas Basin versus Peruvian margin), the most pronounced difference is the MAR_{terr} which is significantly higher in the Guaymas Basin (252 g m^{-2} yr^{-1}; calculated by multiplying the terrigenous content derived in Eq. (1) with the MAR from Eq. (2)) than at the Peruvian margin (100 g m^{-2} yr^{-1}; MAR from Ehlert et al., 2016; terrigenous content calculated after Eq. (1) with 6 wt% $bSiO_2$, 15 wt% OC, 8 wt% $CaCO_3$) (Fig. 5a, b). The high terrigenous detritus content is supplied via rivers in the Guaymas Basin (Calvert, 1966; DeMaster, 1981). In combination with the high MAR_{terr} in the Guaymas OMZ, high water/rock ratios (high porosity) additionally promote dissolution processes (Fig. 5). Lower MAR_{terr} and water/rock ratios found in the Peruvian upwelling margin appear to limit the dissolution rate of terrigenous phases and promote authigenic aluminosilicate precipitation (Fig. 5b, c), shifting pore fluid $\delta^{30}Si_{pf}$ to higher values compared to the corresponding $\delta^{30}Si_{bSiO2}$ and $\delta^{30}Si_{bw}$

values. This illustrates that the pore fluid $\delta^{30}Si_{pf}$ values of apparently similar settings (e.g. OMZ sites) highly depend on the ambient environmental conditions and are not easily transferable.

4.5 Hydrothermal impact on the marine Si cycle

Findings of this study show that additional Si sources like hydrothermal input appear to affect the oceanic $\delta^{30}Si$ values only in close vicinity to the hydrothermal fields. The $\delta^{30}Si$ values of the hydrothermal plume (+0.7 to +1.4‰) are highly diluted by seawater (≥ 94%, Table 2) and thus deviate from hydrothermal fluid $\delta^{30}Si$ values (-0.3‰; De La Rocha et al., 2000). However, the currently available data set regarding $\delta^{30}Si$ values of hydrothermal fluids is limited (two data points; De La Rocha et al., 2000), even though they are in excellent agreement with oceanic crust $\delta^{30}Si$ values (-0.29±; Savage et al., 2010), the rock through which hydrothermal fluids circulate and gain their Si isotopic signature. In our data set, no correlation exists between the $\delta^{30}Si$ values and the Si concentration of the hydrothermal plume (Fig. ~~1S~~S2) and instead the $\delta^{30}Si$ values are predominantly controlled by Si precipitation, likely in the hydrothermal conduit during ascent or after discharge in contact with colder seawater. Temperature variations and interlinked precipitation rates were found in addition to co-precipitation with Al or Fe to cause large Si fractionation such that precipitates are enriched in ^{28}Si (Geilert et al., 2014, 2015; Oelze et al., 2015; Roerdink et al., 2015; Zheng et al., 2016). The varying impacts of these factors can also explain why the diluted hydrothermal plume $\delta^{30}Si$ values with the highest hydrothermal share (Table 2) does not show the lowest $\delta^{30}Si$ values, indicative of hydrothermal fluids, given that Si is more reactive compared to Mg, the element on which the hydrothermal share calculations are based (see supplement from Berndt et al., 2016). The large range in hydrothermal plume $\delta^{30}Si$ values, which clearly show high degrees of seawater dilution, illustrates the complexity of precipitation processes when hydrothermal fluids get in contact with cold seawater and which requires further investigations especially with respect to the impact on the global marine Si cycle.

5. CONCLUSIONS

Marine silicate weathering and reverse weathering impact the pore fluid isotopic composition of sediments and are key processes of the marine Si~~silica~~ cycle. In the Guaymas Basin, these processes have been studied under markedly differing thermal and redox conditions. Si isotope compositions of pore fluids combined with those of biogenic silica and ambient bottom waters helped to decipher marine weathering and reverse weathering reactions, which would have remained undetected by elemental concentrations alone and highlight the importance of Si isotope studies to constrain early

diagenetic reactions. Si concentrations and $\delta^{30}Si_{pf}$ signatures are the result of the interplay between silica dissolution and Si precipitation, however, the involved phases differ significantly between the study sites. Large differences in $\delta^{30}Si_{pf}$ values in a regionally constrained basin show that oxic/anoxic conditions, hydrothermal fluids, water/rock ratios and the input of terrigenous material strongly affect the pathways and turnover rates of Si in marine sediments. The light $\delta^{30}Si_{pf}$ and $\delta^{30}Si_{BW}$ values from the Guaymas OMZ confirm earlier studies suggesting a light Si isotope value of the benthic Si flux (Ehlert et al., 2016; Grasse et al., 2016), which need to be taken into account in future oceanic mass balances of Si and in modelling studies concerning the isotopic Si cycle. Environmental settings, in particular the MARs of terrigenous material, water/rock ratios, and redox conditions appear to be the major factors controlling the balance between marine silicate weathering and reverse weathering and the Si isotope fractionation in pore fluids of marine sedimentary settings and need to be considered particularly in marine Si isotope studies.

AUTHOR CONTRIBUTION

SG, CH, MS, and FS helped sampling and processing of the samples onboard. SG, PG, and KD conducted the Si isotope measurements. SG, CE, PG, KD, FS, and MF helped interpreting the data. KW designed the reactive transport model. SG prepared the manuscript with the contribution of all authors.

COMPETING INTEREST

The authors declare that they have no conflict of interest.

ACKNOWLEDGEMENTS

This work was part of the MAKS project funded by the German Ministry of Science and Education (BMBF). We appreciate the support of the master and crew of the R/V Sonne during the SO241 cruise. We thank Regina Surberg, Bettina Domeyer, and Anke Bleyer for analytical support during the cruise and on shore. Further thanks go to Tabitha Riff, Jutta Heinze, and Tyler Goepfert. Additional support of this work was provided by EU-COST Action ES1301 "FLOWS" (www.flows-cost.eu) and the German Collaborative Research Centre (SFB) 754: Climate – Biogeochemistry Interactions in the Tropical Ocean funded by the German Science Foundation. We would also like to thank an anonymous reviewer, Jill Sutton, and Damien Cardinal for their comments and constructive reviews.

694

695 **References**

696

697 Abrantes, F., Lopes, C., Mix, A. and Pisias, N.: Diatoms in Southeast Pacific surface sediments reflect
698 environmental properties, Quat. Sci. Rev., 26(1–2), 155–169,
699 doi:10.1016/j.quascirev.2006.02.022, 2007.
700 Albarède, F., Telouk, P., Blichert-Toft, J., Boyet, M., Agranier, A. and Nelson, B.: Precise and accurate
701 isotopic measurements using multiple-collector ICPMS, Geochim. Cosmochim. Acta, 68(12),
702 2725–2744, doi:10.1016/j.gca.2003.11.024, 2004.
703 Anderson, T. F. and Raiswell, R.: SOURCES AND MECHANISMS FOR THE ENRICHMENT OF HIGHLY
704 REACTIVE IRON IN EUXINIC BLACK SEA SEDIMENTS, Am. J. Sci., 304, 203–233, 2004.
705 van Bennekom, A. J., Berger, G. . W., Van Der Gaast, S. J. and De Vries, R. T. P.: PRIMARY
706 PRODUCTIVITY AND THE SILICA CYCLE IN THE SOUTHERN OCEAN (ATLANTIC SECTOR),
707 Palaeogeogr. Palaeoclim. Palaeoecol., 67, 19–30, 1988.
708 Berndt, C., Hensen, C., Mortera-Gutierrez, C., Sarkar, S., Geilert, S., Schmidt, M., Liebetrau, V., Kipfer,
709 R., Scholz, F., Doll, M., Muff, S., Karstens, J., Planke, S., Petersen, S., Böttner, C., Chi, W.-C.,
710 Moser, M., Behrendt, R., Fiskal, A., Lever, M. A., Su, C.-C., Deng, L., Brennwald, M. S. and
711 Lizarralde, D.: Rifting under steam – how rift magmatism triggers methane venting from
712 sedimentary basins, Geology, 44(9), 767–770, 2016.
713 Beucher, C. P., Brzezinski, M. A. and Jones, J. L.: Sources and biological fractionation of Silicon
714 isotopes in the Eastern Equatorial Pacific, Geochim. Cosmochim. Acta, 72(13), 3063–3073,
715 doi:10.1016/j.gca.2008.04.021, 2008.
716 Beucher, C. P., Brzezinski, M. A. and Jones, J. L.: Mechanisms controlling silicon isotope distribution in
717 the Eastern Equatorial Pacific, Geochim. Cosmochim. Acta, 75(15), 4286–4294,
718 doi:10.1016/j.gca.2011.05.024, 2011.
719 van den Boorn, S. H. J. M., Vroon, P. Z. and van Bergen, M. J.: Sulfur-induced offsets in MC-ICP-MS
720 silicon-isotope measurements, J. Anal. At. Spectrom., 24(8), 1111, doi:10.1039/b816804k,
721 2009.
722 Bruland, K. W., Rue, E. L., Smith, G. J. and DiTullio, G. R.: Iron, macronutrients and diatom blooms in
723 the Peru upwelling regime: Brown and blue waters of Peru, Mar. Chem., 93(2–4), 81–103,
724 doi:10.1016/j.marchem.2004.06.011, 2005.
725 Calvert, S. E.: Factors affecting distribution of laminated diatomaceous sediments in Gulf of
726 California, in Marine Geology of Gulf of California, edited by T. van Andel and G. G. Shor, pp.
727 311–330, Am Assoc. Petrol. Geol. Mem.3., 1964.
728 Calvert, S. E.: Accumulation of Diatomaceous Silica in the Sediments of the Gulf of California, Geol.

729 Soc. Am. Bull., 77(June), 569–596, 1966.
730 Campbell, A. C. and Gieskes, J. M.: Water column anomalies associated with hydrothermal activity in
731 the Guaymas Basin, Gulf of California Andrew C. Campbell and Joris M. Gieskes, Earth Planet.
732 Sci. Lett., 68, 57–72, 1984.
733 Van Cappellen, P. and Qiu, L. Q.: Biogenic silica dissolution in sediments of the Southern Ocean.1.
734 Solubility, Deep. Res. Part Ii-Topical Stud. Oceanogr., 44(5), 1109–1128, doi:10.1016/S0967-
735 0645(96)00113-0, 1997a.
736 Van Cappellen, P. and Qiu, L.: Biogenic silica dissolution in sediments of the Southern Ocean . II
737 Kinetics, Deep. Res. II, 44(5), 1129–1149, 1997b.
738 Cappelli, C., Yokoyama, S., Cama, J. and Huertas, F. J.: Montmorillonite dissolution kinetics:
739 Experimental and reactive transport modeling interpretation, Geochim. Cosmochim. Acta,
740 227, 96–122, 2018.
741 Cardinal, D., Alleman, L. Y., Dehairs, F., Savoye, N., Trull, T. W. and André, L.: Relevance of silicon
742 isotopes to Si-nutrient utilization and Si-source assessment in Antarctic waters, Global
743 Biogeochem. Cycles, 19(2), 1–13, doi:10.1029/2004GB002364, 2005.
744 Von Damm, K. L.: Seafloor Hydrothermal Activity: Black Smoker Chemistry And Chimneys, Annu. Rev.
745 Earth Planet. Sci., 18(1), 173–204, doi:10.1146/annurev.earth.18.1.173, 1990.
746 Von Damm, K. L., Edmond, J. M., Measures, C. I. and Grant, B.: Chemistry of submarine hydrothermal
747 solutions at Guaymas Basin, Gulf of California, Geochim. Cosmochim. Acta, 49(11), 2221–
748 2237, 1985.
749 Davis, C. C., Chen, H. W. and Edwards, M.: Modeling silica sorption to iron hydroxide, Environ. Sci.
750 Technol., 36(4), 582–587, doi:10.1021/es010996t, 2002.
751 Delstanche, S., Opfergelt, S., Cardinal, D., Elsass, F., André, L. and Delvaux, B.: Silicon isotopic
752 fractionation during adsorption of aqueous monosilicic acid onto iron oxide, Geochim.
753 Cosmochim. Acta, 73(4), 923–934, doi:10.1016/j.gca.2008.11.014, 2009.
754 Demarest, M. S., Brzezinski, M. a. and Beucher, C. P.: Fractionation of silicon isotopes during biogenic
755 silica dissolution, Geochim. Cosmochim. Acta, 73(19), 5572–5583,
756 doi:10.1016/j.gca.2009.06.019, 2009.
757 DeMaster, D. J.: The supply and accumulation of silica in the marine environment., Geochemica
758 Cosmochim. Acta, 45, 1715–1732, 1981.
759 Dixit, S., Van Cappellen, P. and van Bennekom, A. J.: Processes controllong solubility of biogenic silica
760 and pore water build-up of silicic acid in marine sediments, Mar. Chem., 73, 333–352, 2001.
761 Doering, K., Ehlert, C., Grasse, P., Crosta, X., Fleury, S., Frank, M. and Schneider, R.: Differences
762 between mono-generic and mixed diatom silicon isotope compositions trace present and
763 past nutrient utilisation off Peru, Geochim. Cosmochim. Acta, 177, 30–47,

764 doi:10.1016/j.gca.2015.12.029, 2016.
765 Egan, K. E., Rickaby, R. E. M., Leng, M. J., Hendry, K. R., Hermoso, M., Sloane, H. J., Bostock, H. and
766 Halliday, A. N.: Diatom silicon isotopes as a proxy for silicic acid utilisation : A Southern Ocean
767 core top calibration, Geochim. Cosmochim. Acta, 96, 174–192,
768 doi:10.1016/j.gca.2012.08.002, 2012.
769 Ehlert, C., Grasse, P., Mollier-Vogel, E., Böschen, T., Franz, J., de Souza, G. F., Reynolds, B. C.,
770 Stramma, L. and Frank, M.: Factors controlling the silicon isotope distribution in waters and
771 surface sediments of the Peruvian coastal upwelling, Geochim. Cosmochim. Acta, 99, 128–
772 145, doi:10.1016/j.gca.2012.09.038, 2012.
773 Ehlert, C., Grasse, P. and Frank, M.: Changes in silicate utilisation and upwelling intensity off Peru
774 since the Last Glacial Maximum - insights from silicon and neodymium isotopes, Quat. Sci.
775 Rev., 72, 18–35, doi:10.1016/j.quascirev.2013.04.013, 2013.
776 Ehlert, C., Doering, K., Wallmann, K., Scholz, F., Sommer, S., Grasse, P., Geilert, S. and Frank, M.:
777 Stable silicon isotope signatures of marine pore waters – Biogenic opal dissolution versus
778 authigenic clay mineral formation, Geochim. Cosmochim. Acta, 191, 102–117,
779 doi:10.1016/j.gca.2016.07.022, 2016.
780 Frings, P. J., Clymans, W., Fontorbe, G., De La Rocha, C. L. and Conley, D. J.: The continental Si cycle
781 and its impact on the ocean Si isotope budget, Chem. Geol., 425, 12–36,
782 doi:10.1016/j.chemgeo.2016.01.020, 2016.
783 Geilert, S., Vroon, P. Z., Roerdink, D. L., Van Cappellen, P. and van Bergen, M. J.: Silicon isotope
784 fractionation during abiotic silica precipitation at low temperatures: inferences from flow-
785 through experiments, Geochim. Cosmochim. Acta, 142, 95–114,
786 doi:10.1016/j.gca.2014.07.003, 2014.
787 Geilert, S., Vroon, P. Z., Keller, N. S., Gudbrandsson, S., Stefánsson, A. and van Bergen, M. J.: Silicon
788 isotope fractionation during silica precipitation from hot-spring waters: Evidence from the
789 Geysir geothermal field, Iceland, Geochim. Cosmochim. Acta, 164,
790 doi:10.1016/j.gca.2015.05.043, 2015.
791 Geilert, S., Vroon, P. Z. and van Bergen, M. J.: Effect of diagenetic phase transformation on the silicon
792 isotope composition of opaline sinter deposits of Geysir, Iceland, Chem. Geol., 433,
793 doi:10.1016/j.chemgeo.2016.04.008, 2016.
794 Geilert, S., Hensen, C., Schmidt, M., Liebetrau, V., Scholz, F., Doll, M., Deng, L., Fiskal, A., Lever, M. A.,
795 Su, C.-C., Schlömer, S., Sarkar, S., Thiel, V. and Berndt, C.: On the formation of hydrothermal
796 vents and cold seeps in the Guaymas Basin, Gulf of California, Biogeosciences, 15, 5715–5731
797 [online] Available from: https://doi.org/10.5194/bg-15-5715-2018, 2018.
798 Georg, R. B., Reynolds, B. C., Frank, M. and Halliday, A. N.: Mechanisms controlling the silicon

isotopic compositions of river waters, Earth Planet. Sci. Lett., 249(3–4), 290–306, doi:10.1016/j.epsl.2006.07.006, 2006a.

Georg, R. B., Reynolds, B. C., Frank, M. and Halliday, A. N.: New sample preparation techniques for the determination of Si isotopic compositions using MC-ICPMS, Chem. Geol., 235(1–2), 95–104, doi:10.1016/j.chemgeo.2006.06.006, 2006b.

Georg, R. B., Zhu, C., Reynolds, B. C. and Halliday, A. N.: Stable silicon isotopes of groundwater, feldspars, and clay coatings in the Navajo Sandstone aquifer, Black Mesa, Arizona, USA, Geochim. Cosmochim. Acta, 73(8), 2229–2241, doi:10.1016/j.gca.2009.02.005, 2009.

Gieskes, J. M., Kastner, M., Einsele, G., Kelts, K. and Niemitz, J.: Hydrothermal Activity in the Guaymas Basin, Gulf of California: A synthesis, in In Initial Reports of the Deep Sea Drilling Project. vol. 64, Pt. 2, edited by J. Blakeslee, L. W. Platt, and L. N. Stout, pp. 1159–1167., 1982.

Gieskes, J. M., Simoneit, B. R. T., Brown, T., Shaw, T., Wang, Y. C. and Magenheim, A.: Hydrothermal fluids and petroleum in surface sediments of Guaymas Basin, Gulf of California: A case study, Can. Mineral., 26, 589–602 [online] Available from: http://canmin.geoscienceworld.org/cgi/reprint/26/3/589, 1988.

Gieskes, J. M., Gamo, T. and Brumsack, H.: Chemical methods for interstitial water analysis aboard Joides Resolution, Ocean Drill. Prog. Tech. Note 15. Texas A&M Univ. Coll. Stn., 1991.

Golubev, S. V, Bauer, A. and Pokrovsky, O. S.: Effect of pH and organic ligands on the kinetics of smectite dissolution at 25 ° C, Geochim. Cosmochim. Acta, 70, 4436–4451, doi:10.1016/j.gca.2006.06.1557, 2006.

Grasse, P., Ehlert, C. and Frank, M.: The influence of water mass mixing on the dissolved Si isotope composition in the Eastern Equatorial Pacific, Earth Planet. Sci. Lett., 380, 60–71, doi:10.1016/j.epsl.2013.07.033, 2013.

Grasse, P., Ryabenko, E., Ehlert, C., Altabet, M. A. and Frank, M.: Silicon and nitrogen cycling in the upwelling area off Peru: A dual isotope approach, Limnol. Oceanogr., 61(5), 1661–1676, doi:10.1002/lno.10324, 2016.

Grasse, P., Brzezinski, M. A., Cardinal, D., de Souza, G. F., Andersson, P., Closset, I., Cao, Z., Dai, M., Ehlert, C., Estrade, N., François, R., Frank, M., Jiang, G., Jones, J. L., Kooijman, E., Liu, Q., Lu, D., Pahnke, K., Ponzevera, E., Schmitt, M., Sun, X., Sutton, J. N., Thil, F., Weis, D., Wetzel, F., Zhang, A., Zhang, J. and Zhang, Z.: GEOTRACES inter-calibration of the stable silicon isotope composition of dissolved silicic acid in seawater, J. Anal. At. Spectrom., 32(3), 562–578, doi:10.1039/C6JA00302H, 2017.

Hughes, H. J., Delvigne, C., Korntheuer, M., de Jong, J., André, L. and Cardinal, D.: Controlling the mass bias introduced by anionic and organic matrices in silicon isotopic measurements by MC-ICP-MS, J. Anal. At. Spectrom., 26(9), 1892, doi:10.1039/c1ja10110b, 2011.

834 Hurd, D. C.: Interactions of biogenic opal , sediment and seawater in the Central Equatorial Pacific,
835 Geochemica Cosmochim. Acta, 37, 2257–2282, 1973.
836 Kastner, M.: Evidence for Two Distinct Hydrothermal Systems in the Guaymas Basin, in In Initial
837 Reports of the Deep Sea Drilling Project. vol. 64, Pt. 2, edited by J. Blakeslee, L. W. Platt, and
838 L. N. Stout, pp. 1143–1157, U.S. Govt. Printing Office, Washington., 1982.
839 Kastner, M. and Siever, R.: Siliceous Sediments of the Guaymas Basin: The Effect of High Thermal
840 Gradients on Diagenesis, J. Geol., 91(6), 629–641, doi:10.1086/628816, 1983.
841 Köhler, S. J., Bosbach, D. B. and Oelkers, E. H.: Do clay mineral dissolution rates reach steady state?,
842 Geochim. Cosmochim. Acta, 69(8), 1997–2006, doi:10.1016/j.gca.2004.10.015, 2005.
843 De la Rocha, C. L., Brzezinski, M. A. and DeNiro, M. J.: Fractionation of silicon isotopes by marine
844 diatoms during biogenic silica formation, Geochim. Cosmochim. Acta, 61(23), 5051–5056,
845 doi:10.1016/S0016-7037(97)00300-1, 1997.
846 De La Rocha, C. L., Brzezinski, M. A. and Deniro, M. J.: A first look at the distribution of the stable
847 isotopes of silicon in natural waters, Geochim. Cosmochim. Acta, 64(14), 2467–2477,
848 doi:10.1016/S0016-7037(00)00373-2, 2000.
849 Lewin, J. C.: The dissolution of silica from diatom walls, Geochim. Cosmochim. Acta, 21(3–4), 182–
850 198, doi:10.1016/S0016-7037(61)80054-9, 1961.
851 Liu, G., Qiu, S., Liu, B., Pu, Y., Gao, Z., Wang, J., Jin, R. and Zhou, J.: Microbial reduction of Fe(III)-
852 bearing clay minerals in the presence of humic acids, Sci. Rep., 7(9), doi:10.1038/srep45354,
853 2017.
854 Lizarralde, D., Soule, S. A., Seewald, J. S. and Proskurowski, G.: Carbon release by off-axis magmatism
855 in a young sedimented spreading centre, Nat. Geosci., 4(1), 50–54, doi:10.1038/ngeo1006,
856 2010.
857 Loucaides, S., Michalopoulos, P., Presti, M., Koning, E., Behrends, T. and Van Cappellen, P.: Seawater-
858 mediated interactions between diatomaceous silica and terrigenous sediments: Results from
859 long-term incubation experiments, Chem. Geol., 270(1–4), 68–79,
860 doi:10.1016/j.chemgeo.2009.11.006, 2010.
861 Lovley, D. R., Fraga, J. L., Blunt-Harris, E. L., Hayes, L. A., Phillips, E. J. P. and Coates, J. D.: Humic
862 Substances as a Mediator for Microbially Catalyzed Metal Reduction, Acta Hydrochim.
863 hydrobiol, 26, 152–157, 1998.
864 Lupton, J. E.: Helium-3 in the Guaymas Basin: Evidence for injection of mantle volatiles in the Gulf of
865 California, J. Geophys. Res., 84(B13), 7446, doi:10.1029/JB084iB13p07446, 1979.
866 Mackenzie, F. T., Ristvet, B. L., Thorstenson, D. C., Lerman, A. and Leeper, R. H.: Reverse weathering
867 and chemical mass balance in a coastal environment, in River Inputs to Ocean Systems,
868 edited by J. M. Marten, J. D. Burton, and D. Eisma, pp. 152–187, UNEP and UNESCO,

Switzerland., 1981.
McManus, J., Hammond, D. E., Berelson, W. M., Kilgore, T. E., Demaster, D. J., Ragueneau, O. G. and Collier, R. W.: Early diagenesis of biogenic opal: Dissolution rates, kinetics, and paleoceanographic implications, Deep. Res. Part II, 42(2–3), 871–903, doi:10.1016/0967-0645(95)00035-O, 1995.
Méheut, M., Lazzeri, M., Balan, E. and Mauri, F.: Equilibrium isotopic fractionation in the kaolinite, quartz, water system: Prediction from first-principles density-functional theory, Geochim. Cosmochim. Acta, 71(13), 3170–3181, doi:10.1016/j.gca.2007.04.012, 2007.
Michalopoulos, P. and Aller, R. C.: Rapid Clay Mineral Formation in Amazon Delta Sediments: Reverse Weathering and Oceanic Elemental Cycles, Science 270(5236), 614–617, doi:10.1126/science.270.5236.614, 1995.
Michalopoulos, P. and Aller, R. C.: Early diagenesis of biogenic silica in the Amazon delta: Alteration, authigenic clay formation, and storage, Geochim. Cosmochim. Acta, 68(5), 1061–1085, doi:10.1016/j.gca.2003.07.018, 2004.
Michalopoulos, P., Aller, R. C. and Reeder, R. J.: Conversion of diatoms to clays during early diagenesis in tropical, continental shell muds, Geology, 28(12), 1095–1098, doi:10.1130/0091-7613(2000)28<1095:CODTCD>2.0.CO, 2000.
Morley, D. W., Leng, M. J., Mackay, A. W., Sloane, H. J., Rioual, P. and Battarbee, R. W.: Cleaning of lake sediment samples for diatom oxygen isotope analysis, J. Paleolimnol., 31(3), 391–401, doi:10.1023/B:JOPL.0000021854.70714.6b, 2004.
Müller, G.: Methods in sedimentary petrology., in Sedimentary Petrology, Volume 1, edited by W. von Engelhardt, H. Füchtbauer, and G. Müller, pp. 1–283, Schweizerbart, Stuttgart, Germany., 1967.
Müller, P. J. and Schneider, R.: An automated leaching method for the determination of opal in sediments and particulate matter, Deep. Res. Part I, 40(3), 425–444, doi:10.1016/0967-0637(93)90140-X, 1993.
Ng, C. H., Cassarino, L., Pickering, R. A., Woodward, E. M. S., Hammond, S. J. and Hendry, K. R.: Sediment efflux of silicon on the Greenland margin and implications for the marine silicon cycle, Earth Planet. Sci. Lett., 529, 115877, doi:10.1016/j.epsl.2019.115877, 2020.
Oelze, M., von Blanckenburg, F., Bouchez, J., Hoellen, D. and Dietzel, M.: The effect of Al on Si isotope fractionation investigated by silica precipitation experiments, Chem. Geol., 397, 94–105, doi:10.1016/j.chemgeo.2015.01.002, 2015.
Opfergelt, S. and Delmelle, P.: Silicon isotopes and continental weathering processes: Assessing controls on Si transfer to the ocean, Comptes Rendus - Geosci., 344(11–12), 723–738, doi:10.1016/j.crte.2012.09.006, 2012.

Opfergelt, S., Cardinal, D., André, L., Delvigne, C., Bremond, L. and Delvaux, B.: Variations of δ30Si and Ge/Si with weathering and biogenic input in tropical basaltic ash soils under monoculture, Geochim. Cosmochim. Acta, 74(1), 225–240, doi:10.1016/j.gca.2009.09.025, 2010.

Opfergelt, S., Burton, K. W., Pogge von Strandmann, P. A. E., Gislason, S. R. and Halliday, A. N.: Riverine silicon isotope variations in glaciated basaltic terrains: Implications for the Si delivery to the ocean over glacial-interglacial intervals, Earth Planet. Sci. Lett.,(369–370), 211–219, doi:10.1016/j.epsl.2013.03.025, 2013.

Parkhurst, B. D. L. and Appelo, C. A. J.: User's Guide To PHREEQC (version 2) — a Computer Program for Speciation, and Inverse Geochemical Calculations, Exch. Organ. Behav. Teach. J., D(Version 2), 326, doi:Rep. 99-4259, 1999.

Petschick, R., Kuhn, G. and Gingele, F.: Clay mineral distribution in surface sediments of the South Atlantic: sources, transport, and relation to oceanography, Mar. Geol., 130(3–4), 203–229, doi:10.1016/0025-3227(95)00148-4, 1996.

Rabouille, C., Gaillard, J. F., Tréguer, P. and Vincendeau, M. A.: Biogenic silica recycling in surficial sediments across the Polar Front of the Southern Ocean (Indian Sector), Deep. Res. Part II Top. Stud. Oceanogr., 44(5), 1151–1176, doi:10.1016/S0967-0645(96)00108-7, 1997.

Ragueneau, O., Tréguer, P., Leynaert, A., Anderson, R. F., Brzezinski, M. A., DeMaster, D. J., Dugdale, R. C., Dymond, J., Fischer, G., François, R., Heinze, C., Maier-Reimer, E., Martin-Jézéquel, V., Nelson, D. M. and Quéguiner, B.: A review of the Si cycle in the modern ocean: Recent progress and missing gaps in the application of biogenic opal as a paleoproductivity proxy, Glob. Planet. Change, 26(4), 317–365, doi:10.1016/S0921-8181(00)00052-7, 2000.

Rahman, S., Aller, R. C. and Cochran, J. K.: The Missing Silica Sink: Revisiting the Marine Sedimentary Si Cycle Using Cosmogenic 32Si, Global Biogeochem. Cycles, 31(10), 1559–1578, doi:10.1002/2017GB005746, 2017.

Reynolds, B. C., Aggarwal, J., André, L., Baxter, D., Beucher, C., Brzezinski, M. A., Cardinal, D., Engström, E., Georg, R. B., Land, M., Leng, M. J., Opfergelt, S., Rodushkin, I., Sloane, H. J., van den Boorn, S. H. J. M., Vroon, P. Z. and Cardinal, D.: An inter-laboratory comparison of Si isotope reference materials, J. Anal. Atom. Spectrom, 22, 561–568, doi:10.1039/b616755a, 2007.

Reynolds, B. C., Frank, M. and Halliday, A. N.: Evidence for a major change in silicon cycling in the subarctic North Pacific at 2 . 73 Ma, Paleoceanography, 23(PA4219), doi:10.1029/2007PA001563, 2008.

Rickert, D.: Dissolution kinetics of biogenic silica in marine environments, Ber.Polarforschung, 351 [online] Available from: ISSN 0176-5027, 2000.

939 Rickert, D., Schlüter, M. and Wallmann, K.: Dissolution kinetics of biogenic silica from the water
940 column to the sediments, Geochim. Cosmochim. Acta, 66(3), 439–455, doi:10.1016/S0016-
941 7037(01)00757-8, 2002.
942 Roerdink, D. L., van den Boorn, S. H. J. M., Geilert, S., Vroon, P. Z. and van Bergen, M. J.: Experimental
943 constraints on kinetic and equilibrium silicon isotope fractionation during the formation of
944 non-biogenic chert deposits, Chem. Geol., 402, 40–51, doi:10.1016/j.chemgeo.2015.02.038,
945 2015.
946 Savage, P. S., Georg, R. B., Armytage, R. M. G., Williams, H. M. and Halliday, A. N.: Silicon isotope
947 homogeneity in the mantle, Earth Planet. Sci. Lett., 295(1–2), 139–146,
948 doi:10.1016/j.epsl.2010.03.035, 2010.
949 Sayles, F. L., Martin, W. R., Chase, Z. and Anderson, R. F.: Benthic remineralization and burial of
950 biogenic SiO2 , CaCO3 , organic carbon , and detrital material in the Southern Ocean along a
951 transect at 170° West, Deep. Res. Part II, 48, 4323–4383, 2001.
952 Scholz, F., Schmidt, M., Hensen, C., Geilert, S., Gutjahr, M. and Liebetrau, V.: Shelf-to-basin iron
953 shuttle in the Guaymas Basin, Gulf of California, Geochim. Cosmochim. Acta, 261, 76–92,
954 doi:10.1016/j.gca.2019.07.006, 2019.
955 Shemesh, A., Mortlock, R. A., Smith, R. J. and Froelich, P. N.: Determination of Ge/Si in Marine
956 Siliceous Microfossils: Separation, Cleaning and Dissolution of Diatoms and Radiolaria, Mar.
957 Chem., 25, 305–323, 1988.
958 de Souza, G. F., Reynolds, B. C., Rickli, J., Frank, M., Saito, M. A., Gerringa, L. J. A. and Bourdon, B.:
959 Southern Ocean control of silicon stable isotope distribution in the deep Atlantic Ocean,
960 Global Biogeochem. Cycles, 26(2), 1–13, doi:10.1029/2011GB004141, 2012.
961 de Souza, G. F., Slater, R. D., Dunne, J. P. and Sarmiento, J. L.: Deconvolving the controls on the deep
962 ocean's silicon stable isotope distribution, Earth Planet. Sci. Lett., 398, 66–76,
963 doi:10.1016/j.epsl.2014.04.040, 2014.
964 de Souza, G. F., Slater, R. D., Hain, M. P., Brzezinski, M. A. and Sarmiento, J. L.: Distal and proximal
965 controls on the silicon stable isotope signature of North Atlantic Deep Water, Earth Planet.
966 Sci. Lett., 432, 342–353, doi:10.1016/j.epsl.2015.10.025, 2015.
967 Sutton, J. N., Varela, D. E., Brzezinski, M. A. and Beucher, C. P.: Species-dependent silicon isotope
968 fractionation by marine diatoms, Geochim. Cosmochim. Acta, 104, 300–309,
969 doi:10.1016/j.gca.2012.10.057, 2013.
970 Sutton, J. N., André, L., Cardinal, D., Conley, D. J., de Souza, G. F., Dean, J., Dodd, J., Ehlert, C.,
971 Ellwood, M. J., Frings, P. J., Grasse, P., Hendry, K., Leng, M. J., Michalopoulos, P., Panizzo, V.
972 N. and Swann, G. E. A.: A Review of the Stable Isotope Bio-geochemistry of the Global Silicon
973 Cycle and Its Associated Trace Elements, Front. Earth Sci., 5(January),

974 doi:10.3389/feart.2017.00112, 2018.
975 Tatzel, M., von Blanckenburg, F., Oelze, M., Schuessler, J. A. and Bohrmann, G.: The silicon isotope
976 record of early silica diagenesis, Earth Planet. Sci. Lett., 428, 293–303,
977 doi:10.1016/j.epsl.2015.07.018, 2015.
978 Teske, A., Callaghan, A. V. and LaRowe, D. E.: Biosphere frontiers of subsurface life in the sedimented
979 hydrothermal system of Guaymas Basin, Front. Microbiol., 5(JULY), 1–11,
980 doi:10.3389/fmicb.2014.00362, 2014.
981 Thunell, R. C., Pride, C. J., Tappa, E. and Muller-Karger, F. E.: Biogenic silica fluxes and accumulation
982 rates in the Gulf of California, Geology, 22, 303–306, doi:10.1130/0091-
983 7613(1994)022<0303, 1994.
984 Tréguer, P. and Pondaven, P.: Silica control of carbon dioxide, Nature, 406, 358–359,
985 doi:10.1080/00207238608710255, 2000.
986 Tréguer, P. J. and De La Rocha, C. L.: The World Ocean Silica Cycle, Ann. Rev. Mar. Sci., 5(1),
987 120725114348000, doi:10.1146/annurev-marine-121211-172346, 2013.
988 Varela, D. E., Pride, C. J. and Brzezinski, M. A.: Biological fractionation of silicon isotopes in Southern
989 Ocean surface waters, Global Biogeochem. Cycles, 18(1), 1–8, doi:10.1029/2003GB002140,
990 2004.
991 Viers, J., Dupré, B. and Gaillardet, J.: Chemical composition of suspended sediments in World Rivers :
992 New insights from a new database, Sci. Total Environ., 407(2), 853–868,
993 doi:10.1016/j.scitotenv.2008.09.053, 2009.
994 Vogt, C., Lauterjung, J. and Fischer, R. X.: INVESTIGATION OF THE CLAY FRACTION (<2µm) OF THE
995 CLAY MINERALS SOCIETY REFERENCE CLAYS, Clays Clay Miner., 50(3), 388–400, 2002.
996 Wallmann, K., Aloisi, G., Haeckel, M., Tishchenko, P., Pavlova, G., Greinert, J., Kutterolf, S. and
997 Eisenhauer, A.: Silicate weathering in anoxic marine sediments, Geochim. Cosmochim. Acta,
998 72(12), 2895–2918, doi:10.1016/j.gca.2008.03.026, 2008.
999 Wetzel, F., de Souza, G. F. and Reynolds, B. C.: What controls silicon isotope fractionation during
1000 dissolution of diatom opal?, Geochim. Cosmochim. Acta, 131, 128–137,
1001 doi:10.1016/j.gca.2014.01.028, 2014.
1002 Zambardi, T. and Poitrasson, F.: Precise Determination of Silicon Isotopes in Silicate Rock Reference
1003 Materials by MC-ICP-MS, Geostand. Geoanalytical Res., 35(1), 89–99, doi:10.1111/j.1751-
1004 908X.2010.00067.x, 2011.
1005 Zheng, X., Beard, B. L., Reddy, T. R., Roden, E. E. and Johnson, C. M.: Abiologic silicon isotope
1006 fractionation between aqueous Si and Fe(III)-Si gel in simulated Archean seawater :
1007 Implications for Si isotope records in Precambrian sedimentary rocks, Geochemica
1008 Cosmochim. Acta, 187, 102–122, 2016.

Ziegler, K., Chadwick, O., Brzezinski, M. and Kelly, E. F.: Natural variations of δ30Si ratios during progressive basalt weathering, Hawaiian Islands, Geochim. Cosmochim. Acta, 69(19), 4597–4610, doi:10.1016/j.gca.2005.05.008, 2005a.

Ziegler, K., Chadwick, O., White, A. F. and Brzezinski, M.: δ30Si systematics in a granitic saprolite, Puerto Rico, Geology, 33(10), 817–820, doi:10.1130/G21707.1, 2005b.

Tables

Table 1: Pore fluid Si concentration (µM), $\delta^{30}Si_{pf}$ values (‰) as well as biogenic silica weight fraction ($bSiO_2$ in wt%), Al/Si ratio (mM/M), $\delta^{30}Si_{bSiO2}$ values (‰), porosity (Ø), Al and K contents (wt%) for the basin sites, hydrothermal site, and OMZ site.

Table 2: Water column and hydrothermal plume Si concentration (µM) and Si isotope values (‰). Additionally, the share of hydrothermal fluids within the hydrothermal plume is given based on the calculation provided by Berndt et al. (2016) in their supplementary materials.

Figures

Fig. 1. A) Location map of the sampling stations in the Guaymas Basin, Gulf of California. Black square in the overview map indicates the sampling area. B) Sedimentary $bSiO_2$ content at each sampling station. Water column stations were above MUC15-02 (VCTD02) in the basin, the hydrothermal site (VCTD06, 09), and at the OMZ site (VCTD07).

Fig 2: Depth (cmbsf) profiles for all stations for pore fluid Si concentration ($Si(OH)_4$) in µM (grey symbols) and $\delta^{30}Si_{pf}$ values (colored symbols) and biogenic opal weight fraction ($bSiO_2$) in wt% (grey symbols) and $\delta^{30}Si_{bSiO2}$ values (colored symbols). The dashed line is the $\delta^{30}Si$ value of the deep basin (VCTD02) and the dotted line represents the $\delta^{30}Si$ value of the water column in the OMZ (VCTD07). The uppermost Si isotope data point in the pore fluid diagrams refers to the bottom water (labelled BW). Note the different depth scale for the OMZ site. The brackets around the MUC22-04 bottom water Si concentration value indicate possible surface water contamination. Error bars not indicated are within symbol size. The long-term error (2SD) of international standards is indicated in the upper right $\delta^{30}Si_{pf}$-depth profile.

Fig. 3. Pore fluid $\delta^{30}Si$ values are displayed versus the inverse Si concentration (1/Si) for the basin sites, the hydrothermal site, and the OMZ site. Error bars not indicated are within symbol size. Mixing curves are calculated after Eq. (3) between the respective water column and the average $bSiO_2$ $\delta^{30}Si$ value for all sites (see text for details). The grey shaded area indicates the uncertainty on the equilibrium solubility of $bSiO_2$ assuming 900±150µM following (Van Cappellen and Qiu, (1997a).

Fig. 4. Asymptotic Si concentration (a) and the pore fluid $\delta^{30}Si_{pf}$ values (b) as a function of the terrigenous/$bSiO_2$ ratio for the basin sites, the hydrothermal site, and the OMZ site in the Guaymas Basin. An exponential increase in Sisilicate concentrations with decreasing terrigenous/$bSiO_2$ ratio is observed, which is not reflected by corresponding systematic changes in $\delta^{30}Si_{pf}$. The values for the terrigenous/$bSiO_2$ ratio defining the global trend (grey dots) are from the Southern Ocean, Scotia Sea, Norwegian Sea, NE Atlantic, Juan de Fuca Ridge, Arabian Sea, and the Peru Basin (Van Cappellen and Qiu, 1997a; Rabouille et al., 1997; Rickert, 2000).

Fig. 5. Conceptual model of the processes influencing pore fluid $\delta^{30}Si_{pf}$ values in the Guaymas Basin (a) and the Peruvian margin after (Ehlert et al., (2016) (b). Bold values in the sediment show the average pore fluid $\delta^{30}Si_{pf}$ values. Arrow length indicates the dominating process (dissolution versus precipitation). The $\delta^{30}Si$ values in the hydrothermal plume indicate dilution with seawater (see section 4.5). (c) The average pore fluid $\delta^{30}Si_{pf}$ values are shown, indicating the dominance of precipitation or dissolution processes for the three settings in the Guaymas Basin and the Peruvian OMZ.

Fig. 6. Data and model results for OMZ core. a: Porosity. b: Biogenic opal concentration in solid phase. c: K/Al ratio in solid phase. d: Dissolved Sisilica concentration in pore fluids. e: Dissolved potassium in pore fluids. f: Isotopic composition of dissolved Sisilica. g: rate of biogenic opal dissolution. h: Rate of authigenic phase precipitation. i: Rate of terrigenous phase dissolution. Sensitivity tests of the model are indicated by setting the dissolution of terrigenous clay phases to zero (red dashed line) and setting the precipitation of authigenic phases to zero (black dashed line). The model values agree best to the measured data when both processes take place (blue line, best fit).